Deciphering the potential niche of two novel black yeast fungi from a biological soil crust based on their genomes, phenotypes, and melanin regulation

Erin C. Carr[1], Quin Barton[2], Sarah Grambo[3], Mitchell Sullivan[1], Cecile M. Renfro[4], Alan Kuo[5], Jasmyn Pangilinan[5], Anna Lipzen[5], Keykhosrow Keymanesh[5], Emily Savage[5], Kerrie Barry[5], Igor V. Grigoriev[5,6], Wayne R. Riekhof[1], Steven D. Harris[7,8]

1) University of Nebraska-Lincoln, School of Biological Sciences, Lincoln, Nebraska 68588; 2) University of Nebraska-Lincoln, Department of Biochemistry, Lincoln, Nebraska 68588; 3) Iowa State University, Roy J. Carver Department of Biochemistry, Biophysics, and Molecular Biology, Ames, Iowa 50011; 4) University of Nebraska-Lincoln, Department of Agronomy and Horticulture, Lincoln, Nebraska 68588; 5) US Department of Energy Joint Genome Institute Lawrence Berkley National Laboratory, Berkley California 94720; 6) Department of Plant and Microbial Biology, University of California Berkeley, Berkeley, California 94720; 7) Iowa State University, Department of Plant Pathology and Microbiology, Ames, Iowa 50011; 8) Iowa State University, Department of Entomology Ames, Iowa 50011

Abstract

Black yeasts are polyextremotolerant fungi that contain high amounts of melanin in their cell wall and maintain a primarily yeast form. These fungi grow in xeric, nutrient deplete environments which implies that they require highly flexible metabolisms and the ability to form lichen-like mutualisms with nearby algae and bacteria. However, the exact ecological niche and interactions between these fungi and their surrounding community is not well understood. We have isolated two novel black yeast fungi of the genus *Exophiala*: *E. viscosium* and *E. limosus*, which are from dryland biological soil crusts. A combination of whole genome sequencing and various phenotyping experiments have been performed on these isolates to determine their fundamental niches within the biological soil crust consortium. Our results reveal that these *Exophiala* spp. are capable of utilizing a wide variety of carbon and nitrogen sources potentially from symbiotic microbes, they can withstand many abiotic stresses, and can potentially provide UV resistance to the crust community in the form of secreted melanin. Besides the identification of two novel species within the genus *Exophiala*, our study also provides new insight into the production and regulation of melanin in extremotolerant fungi.

Background

Polyextremotolerant fungi are a polyphyletic group that can be divided morphologically into black yeast and microcolonial/meristematic fungi types (Gostinčar et al., 2012). These two sub-types are distinct in their morphology; black yeast fungi are usually only yeasts but can be dimorphic, whereas microcolonial fungi are typically filamentous, pseudohyphal, or possess other unique morphologies such as spherical cells (Ametrano et al., 2017; De Hoog et al., 2003; Gostinčar et al., 2011). However, all polyextremotolerant fungi share the capacity to produce melanin, which presumably accounts for much of their polyextremotolerance. Most polyextremotolerant fungi are in the subdivision Pezizomycotina, residing mainly within Eurotiomycetes and Dothidiomycetes, but one could argue that any fully melanized fungus could be a polyextremotolerant fungi (Gostinčar et al., 2009).

Melanin is arguably a defining feature of polyextremotolerant fungi given that they form unmistakably black colonies. Because of its structure and association with the cell wall, melanin imbues polyextremotolerant fungi with resistance to multiple forms of stress. Most commonly known is

ultraviolet (UV) light resistance, as melanin absorbs light in the UV part of the spectrum (Kobayashi et al., 1993). However, melanin is also capable of absorbing reactive oxygen species (ROS), reactive nitrogen species (RNS), providing tolerance to toxic metals, reducing desiccation, and potentially using ionizing radiation as an energy source (Cordero & Casadevall, 2017; Dadachova et al., 2007; Gessler et al., 2014; Płonka & Grabacka, 2006; Zanne et al., 2020). Collectively, these functions of melanin are thought to enhance the ability of polyextremotolerant fungi to colonize habitats that are otherwise inhospitable to most forms of life.

The production of melanin is a key functional trait observed in fungi spanning the fungal kingdom (Bell & Wheeler, 1986; Zanne et al., 2020). The diverse protective functions of melanin (e.g., metal resistance, ROS and RNS tolerance, UV resistance) underscores its broad utility in mitigating the impacts of stress despite the potential cost of its synthesis (Schroeder et al., 2020). Fungi are capable of producing three different types of melanin: pheomelanin, allomelanin, and pyomelanin, all of which have their own independent biosynthetic pathways (Pal et al., 2014; Perez-Cuesta et al., 2020). Allomelanin, is formed from the polymerization of 1,8-DHN, which requires the use of polyketide synthase for initial steps in production (Perez-Cuesta et al., 2020; Płonka & Grabacka, 2006) (**Figure 1**). Pyomelanin and pheomelanin share an initial substrate of Tyrosine, but pheomelanin derives from L-DOPA, whereas pyomelanin is created via tyrosine degradation (Perez-Cuesta et al., 2020; Płonka & Grabacka, 2006) (**Figure 1**). Allomelanin and pheomelanin are often referred to as DHN melanin and DOPA melanin respectively, given their chemical precursors. Unfortunately, due to the unique characteristics of melanins and their association with larger biomolecules, we do not know the complete structure of any type of melanin (Cao et al., 2021). However, given that we do know their chemical constituents, it is possible to draw some inferences about the relationship between structure and function of a particular type of melanin. For instance, out of the three types of melanin fungi can produce, only pheomelanin has a chemical precursor, 5-CysDOPA, with both Nitrogen and Sulfur in its structure (Płonka & Grabacka, 2006). Notably, all three fungal melanins are synthesized via independent pathways, which enables the targeted use of chemical inhibitors to block one pathway without interfering with the others. For example, previous studies have extensively used the chemical melanin blockers kojic acid and phthalide to block pheomelanin and allomelanin respectively (Pal et al., 2014) (**Figure 1**). Use of these chemical blockers allowed previous studies to identify the primary melanin biosynthetic pathway employed by individual fungal species (Pal et al., 2014).

Polyextremotolerant fungi tend to occupy extreme niches such as rock surfaces, external brick and marble walls, soil surfaces, and even the inside of dishwashers (Gostinčar et al., 2009; Zupančič et al., 2016). Characteristic features of these environments includes the relative paucity of nutrients and the frequent presence of a community biofilm consisting of photosynthetic organisms and/or bacteria (Gostinčar et al., 2012). Strikingly, these species are rarely found alone in their habitats, which suggests that multi-species interactions between fungi, bacteria, and photosynthetic organisms underlie the formation and function of these communities. That is, the ability of polyextremotolerant fungi to successfully adapt to their niche must depend on complex yet poorly understood interactions with other microbes.

We have isolated two polyextremotolerant fungi from a biological soil crust (BSC) in B.C., Canada. These novel fungi are of the genus *Exophiala*, which has previously been found in BSCs (Bates et al., 2006). Biological soil crusts are unique dryland biofilms that form on the surface of xeric desert soils where little to no plants are able to grow (Belnap, 2003; Belnap et al., 2001). They are notable for their

extensive cyanobacteria population, which seeds the initial formation of all biological soil crusts and creates the main source of nitrogen for the rest of the community (Belnap, 2002). Once the initial crust is established, it is then inundated with a consortium of bacteria, fungi, algae, archaea, lichens, and mosses (Bates et al., 2010; Lan et al., 2012; Maier et al., 2016). This community is a permanent fixture on the land they occupy unless physically disturbed, much like other biofilms (Belnap & Eldridge, 2001; Donlan & Costerton, 2002). As a result of the desert conditions BSCs reside in, the microbes found there are constantly exposed to extreme abiotic factors which they must tolerate simultaneously (Bowker et al., 2010). Some of these abiotic extremes are: UV radiation (especially at higher altitudes and closer to the poles) (Bowker et al., 2002), desiccation and osmotic pressures (Rajeev et al., 2013), and temperature fluctuations both daily and annually (Belnap et al., 2001; Bowker et al., 2002; Pócs, 2009). Microbes that reside in these biological soil crusts have therefore adapted mechanisms to withstand these abiotic extremes.

An extensive amount of research has been dedicated to certain members of the biological soil crust community, but one such less studied microbe has been the "free-living" fungal taxa. These fungi are non-lichenized (Teixeira et al., 2017) yet are still thriving in an environment where there are no plants to infect or decompose (Belnap & Lange, 2003), and no obvious source of nutrients besides contributions from the other members of the biological soil crust community (Belnap & Lange, 2003). This would imply that even though these fungi are not lichenized per say, they would have to be engaging in lichen-like interactions with the biological soil crust community to obtain vital nutrients for proliferation. While the idea of transient interactions between non-lichenized fungi and other microbes has been floated by previous researchers in other systems (Gostinčar et al., 2012; Grube et al., 2015; Hom & Murray, 2014), it will be a difficult task to strongly confirm in biological soil crusts given their taxonomic complexity.

Despite the importance of microbial interactions in enabling the successful formation of BSCs in a niche characterized by poor nutrient and water availability, the fungal components of BSCs and their relative functions within the interaction network remain poorly understood. Here, we combine genome sequencing with computational tools and culture-based phenotyping to describe two new species of black yeast fungi associated with BSCs. We report on their carbon and nitrogen utilization profiles, stress responses, and lipid accumulation patterns. In addition, we characterize their capacity for melanin production and generate valuable insight into mechanisms that might be involved in regulating the synthesis of these compounds and how their melanin production contributes to the BSC community.

Methods

Fungal Strains and Media

Two novel species of fungi are described here: *Exophiala viscosium* CBS 148801 and *Exophiala limosus* CBS 148802. Their genomes and transcriptomes are deposited at the Department of Energy's (DOE) Joint Genome Institute (JGI) on their Mycocosm website under their genus species names, and the National Center for Biotechnological Information (NCBI) under accession numbers PRJNA501636 for *E. viscosium* and PRJNA501637 for *E. limosus.* Their type strains have been deposited to the Westerdijk institute for access to the scientific community. *E. viscosium* and *E. limosus* are typically grown in malt extract medium (MEA; see **Table 1** for media recipe) at room temperature in an Erlenmeyer flask at 1/10th the volume of the flask, shaking at 200 rpm. Additional strains used in this study were *Saccharomyces cerevisiae* ML440 and BY4741, and *E. dermatitidis* wild type (WT) strain ATCC 34100. *S.*

125 *cerevisiae* strains are grown in Yeast Peptone Dextrose medium (YPD; see **Table 1** for media recipe), and
126 *E. dermatitidis* is grown in MEA.

127 *Fungal isolation and identification methods*

128 Fungi were isolated from public land in B.C., Canada. Soil samples were taken from the top 2 cm of
129 biological soil crusts. A 0.1 g portion of the crust was re-suspended in 1 mL of water, ground with a
130 sterile micropestle, and diluted with a dilution factor (DF) of 10 till they reached 10,000x dilution. Each
131 dilution was then spread out onto two different MEA petri plate containing either no antibiotics or
132 containing: Ampicillin (100 mg/L), Chloramphenicol (50 mg/L), Gentamycin (10 mg/L), and
133 Cycloheximide (100 mg/L). The plates were then incubated in a Percival light incubator at 23 °C with a 12
134 hr light/dark cycle and examined daily using a dissection microscope to check for small black colonies.
135 Once a potential black colony was seen, half of it was removed and transferred to a new MEA (no
136 antibiotics) petri plate. It was vital to examine the plates daily, because even in the presence of
137 antibiotics many unwanted fast-growing microbes would grow on the plates and cover up the slower
138 growing polyextremotolerant fungal colonies. Once a pure culture of each isolate was grown up
139 (approximately 2 weeks), they were preserved in 30% Glycerol and stored in the -80 °C freezer. DNA
140 sequencing of amplified internal transcribed spacer (ITS) sequences was used to identify the isolates.
141 DNA was extracted using the Qiagen DNeasy Powersoil DNA extraction kit. Primers used to isolate the
142 ITS region were: ITS1- (5'-TCC GTA GGT GAA CCT GCG G-3') and ITS4- (5'-TCC TCC GCT TAT TGA TAT GC-
143 3') (White et al., 1990). A BioRad MJ Mini Personal Thermal Cycler was used, with the program set as: 1)
144 95 °C for 5:00 (5 minutes), 2) 94 °C for 0:30 (30 seconds), 3) 55 °C for 0:30, 4) 72 °C for 1:30, 5) Return to
145 2 35 times, 6) 72 °C for 5:00. Resulting PCRs were then checked via gel electrophoresis in 1% agar run at
146 80 V for 1 hr. Isolated ITS regions were sequenced using the Eurofins sequencing facility, and the
147 sequences were subsequently identified using the basic locally aligned search tool (BLAST) of the
148 National Center for Biotechnological Information (NCBI) database to look for potential taxa matches.

149 *DNA extraction and RNA extraction for whole genome sequencing*

150 A Cetyltrimethylammonium bromide (CTAB) based DNA extraction method was performed to obtain
151 high molecular weight DNA for whole genome sequencing. The DNA extraction method used was
152 derived from (Cubero et al., 1999). Changes to the original protocol include switching PVPP for the same
153 concentration of PVP, use of bead beating tubes with liquid nitrogen-frozen cells and the extraction
154 buffer instead of a mortar and pestle for breaking open the cells, and heating up the elution buffer to 65
155 °C before eluting the final DNA. These changes were made to optimize the protocol for liquid-grown
156 yeast cells instead of lichen material. Cells for the DNA extraction were grown up in 25 mL of liquid MEA
157 in 250 mL Erlenmeyer flasks for 5 days, 1 mL of those grown cells was used for the DNA extraction after
158 washing with water twice.

159 RNA was obtained using the Qiagen RNeasy mini kit (Cat. No. 74104). Cells were grown in 25 mL of three
160 different liquid media types (MEA, YPD, and MNV; see **Table 1**) in 250 mL Erlenmeyer flasks at room
161 temperature for 5 days, and 1-2 mL of cells were used for the RNA extraction. Cells were washed with
162 DEPC-treated water and flash frozen in liquid nitrogen in 1.5 mL microcentrifuge tubes. RNA extraction
163 was then performed according to the methods by the RNeasy kit.

164

165 *Genome assembly and annotation*

166 Both genomes and transcriptomes were sequenced using Illumina technology. For transcriptomes, a
167 plate-based RNA sample prep was performed on the PerkinElmer Sciclone next generation sequencing
168 (NGS) robotic liquid handling system using Illuminas TruSeq Stranded mRNA high throughput (HT)
169 sample prep kit utilizing poly-A selection of mRNA following the protocol outlined by Illumina in their
170 user guide: https://support.illumina.com/sequencing/sequencing_kits/truseq-stranded-mrna.html, and
171 with the following conditions: total RNA starting material was 1 µg per sample and 8 cycles of PCR was
172 used for library amplification. The prepared libraries were quantified using KAPA Biosystems' next-
173 generation sequencing library qPCR kit and run on a Roche LightCycler 480 real-time PCR instrument.
174 The libraries were then multiplexed and prepared for sequencing on the Illumina NovaSeq sequencer
175 using NovaSeq XP v1 reagent kits, S4 flow cell, following a 2x150 indexed run recipe.

176 Using BBDuk (https://sourceforge.net/projects/bbmap/), raw reads were evaluated for artifact
177 sequence by kmer matching (kmer=25), allowing 1 mismatch and detected artifact was trimmed from
178 the 3' end of the reads. RNA spike-in reads, PhiX reads and reads containing any Ns were removed.
179 Quality trimming was performed using the phred trimming method set at Q6. Finally, following
180 trimming, reads under the length threshold were removed (minimum length 25 bases or 1/3 of the
181 original read length - whichever is longer). Filtered reads were assembled into consensus sequences
182 using Trinity ver. 2.3.2 (Grabherr et al., 2011).

183 For genomes, DNA library preparation for Illumina sequencing was performed on the PerkinElmer
184 Sciclone NGS robotic liquid handling system using Kapa Biosystems library preparation kit. 200 ng of
185 sample DNA was sheared to 300 bp using a Covaris LE220 focused-ultrasonicator. The sheared DNA
186 fragments were size selected by double-SPRI and then the selected fragments were end-repaired, A-
187 tailed, and ligated with Illumina compatible sequencing adaptors from IDT containing a unique
188 molecular index barcode for each sample library. The prepared libraries were quantified using KAPA
189 Biosystems' next-generation sequencing library qPCR kit and run on a Roche LightCycler 480 real-time
190 PCR instrument. The quantified libraries were then multiplexed with other libraries, and the pool of
191 libraries was then prepared for sequencing on the Illumina HiSeq sequencing platform utilizing a TruSeq
192 paired-end cluster kit, v4, and Illumina's cBot instrument to generate a clustered flow cell for
193 sequencing. Sequencing of the flow cell was performed on the Illumina HiSeq2500 sequencer using
194 HiSeq TruSeq SBS sequencing kits, v4, following a 2x150 indexed run recipe.

195 An initial assembly of the target genome was generated using VelvetOptimiser version 2.1.7 (3) with
196 Velvet version 1.2.07 (Zerbino & Birney, 2008) using the following parameters; "--s 61 --e 97 --i 4 --t 4, --
197 o "-ins_length 250 -min_contig_lgth 500"". The resulting assembly was used to simulate 28X of a 2x100
198 bp 3000 +/- 300bp insert long mate-pair library with wgsim version 0.3.1-r13
199 (https://github.com/lh3/wgsim) using "-e 0 -1 100 -2 100 -r 0 -R 0 -X 0 -d 3000 -s 30". 25X of the
200 simulated long mate-pair was then co-assembled together with 125X of the original Illumina filtered
201 fastq with AllPathsLG release version R49403 (Gnerre et al., 2011) to produce the final nuclear
202 assembly. The genome was annotated using JGI Annotation pipeline (Grigoriev et al., 2013). The
203 assemblies and annotations of both genomes are available at the fungal genome portal MycoCosm
204 ((Grigoriev et al., 2013); https://mycocosm.jgi.doe.gov) and in the DDBJ/EMBL/GenBank repository
205 under accessions PRJNA501636 and PRJNA501637.

206 *Phylogenetic analysis*

207 Our approximate maximum likelihood phylogenetic tree was constructed from the protein sequences of
208 24 taxa which represent a sampling of the family Herpotrichielleaceae in which *E. viscosium* and *E.*
209 *limosus* reside. We created this tree using the pipeline described in Kuo et al. (Kuo et al., 2014). We
210 wanted to obtain the largest set of data for phylogenetic analysis available by defining homologous
211 proteins across all 24 genomes using Best Bidirectional Blast pairs via BlastP across all proteins of all the
212 genomes from their FilteredModels or ExternalModels files available on Mycocsm. Resulting defined
213 homologous proteins across all 24 genomes were then used as our sequences for the rest of the
214 pipeline. These sequences were aligned with Mafft v7.123b with no alterations (Katoh et al., 2002). That
215 alignment was then trimmed using Gblocks 0.91b with options -b4=5 -b5=h to have a minimum of 5
216 positions per block and allowing up to half of those to be gaps (Castresana, 2000). The resulting trimmed
217 alignment was then input into FastTree version 2.1.5 SSE3 with options -gamma -wag (Price et al., 2009).
218 The tree file was then input into iTOL for visual optimization (Letunic & Bork, 2021).

219 *Mating type locus identification*

220 Mating loci for *E. viscosium* and *E. limosus* were determined using the methods described by (Teixeira et
221 al., 2017). Genes known to flank the MAT loci of most Chaetothyriales species include: *APN2*, *SLA2*,
222 *APC5*, and *COX13*. The protein sequences of these genes from *Aspergillus nidulans* were used to BLASTP
223 against the genomes of the new fungi. These gene sequences were obtained from Aspergillus Genome
224 Database and BLASTed using JGI's Mycocosm. Once those genes were found, analysis of upstream and
225 downstream flanking genes was performed until the mating gene MAT1-1 was located. Genes close to
226 MAT1-1 and within the span of genes listed above were considered part of the MAT locus.

227 Phenotyping experiments:

228 Characterization of *E. viscosium* and *E. limosus* was performed to provide us with the knowledge of
229 these new species' capabilities. Experiments performed were carbon utilization, nitrogen utilization, UV
230 resistance, metal resistance, growth temperature range, budding patterns, lipid profiles, and growth
231 capabilities on various fungal medias as described below.

232 *Budding Pattern determination*

233 Protocols for observing the budding patterns of these new species were derived from methods in
234 (Mitchison-Field et al., 2019). A 1:1:1 ratio by weight of Vaseline, Parafin, and Lanolin (VALAP) was
235 combined in a glass bottle and heated to 115 °C to melt completely and kept at room temperature for
236 later use. Heated solid MEA was aliquoted into a 50mL tube for agar slab making. Isolates were grown in
237 liquid MEA for 5 days prior to inoculation of slides. First, the VALAP was brought back up to 115 °C to
238 melt completely for application. Then 5 µL of the 5-day old cells were diluted in 995 µL of liquid MEA.
239 Agar slabs of MEA were made by microwaving the 50 mL tube of solid MEA until it melted, then
240 pipetting 1 mL of the hot agar into a 1 cm x 2 cm mold formed out of cut strips of silicone and laid down
241 in a sterile petri dish. This agar slab was allowed to solidify and was then cut in half to be 1 cm x 1 cm.
242 Both the cover slip and the slide were wiped down with ethanol to ensure clean and sterile growth
243 conditions for the cells. 8 µL of the diluted cells was pipetted onto the center of the sterile slide, then
244 one square of the agar slab was carefully placed on top of the cells in media, 8 µL of MEA was pipetted
245 onto the top of the agar slab, and the coverslip was placed over the agar slab. Using a small paintbrush,
246 the melted VALAP was carefully painted onto the gap between the coverslip and the microscope slide to

247 seal off the coverslip. Finally, a 23-gauge needle was used to poke holes in the solidified VALAP to allow
248 for gas exchange.

249 The slide was then placed with the slide facing down onto the inverted microscope EVOS fl. Once an
250 adequate number of cells was observed in frame, the cells were allowed to settle for 2 hours before
251 imaging began. Images were then automatically taken every 30 mins for 72 hours. Videos of the budding
252 pattern were created using Adobe Premiere Pro.

253 *Growth of E. viscosium and E. limosus on different medias*

254 Eight different fungal media were used to observe the growth of these novel fungi. These media have
255 been used for identification purposes and will be useful for future identification of these species from
256 other locations. Media used in this experiment were: MAG, MEA, MN, MNV, MN+NAG, PDA, Spider,
257 YPD, V8 (**Table 1**). Both isolates were first grown in 25 mL of liquid MEA at room temperature, shaking at
258 200 rpm for 5 days. Then 1 mL of each species was aliquoted and washed 3 times with water. Washed
259 cells were then applied to the media in three ways: 5 µL spotting (pipetting 5 µL of cells onto the plate),
260 toothpick poking (poking a sterile toothpick tip into the suspended cells and then onto a plate), and
261 metal loop streaking (placing sterile metal loop into suspended cells, then spreading cells onto plate in a
262 decreasing manner). This provided us with different plating techniques that could potentially yield
263 different morphologies.

264 *Carbon Utilization*

265 Carbon utilization of each isolate was determined using a BioMerieux ID C32 carbon utilization strip (Cat.
266 No. 32200-1004439110). These strips have 30 different carbon sources in individual wells, one well with
267 no carbon source for a negative control, and one well with Ferric citrate. The inoculated strips were kept
268 in a plastic box container with a lid and lined with moist paper towels to reduce drying. The initial
269 inoculum of cells was prepared in 25 mL of MEA shaking at room temp for 5 days. Inoculation of the
270 strips was done according to the instructions provided by the vendor, and each strain was inoculated in
271 three separate strips for triplicate replication. Cells were diluted to the kit requirement of McFarland
272 standard #3 (McFarland, 1907) before starting the inoculum. Growth in the ID strip lasted 10 days
273 before evaluation. Growth in each well was observed and evaluated by eye. Each well was compared to
274 the negative control (no carbon) and the positive control (dextrose). Initial growth was evaluated on a:
275 +, V, -, and - - scale. If a well had the same growth as the negative control it was given a "-", meaning no
276 growth; if the well had less growth than the negative control it was given a "- -", meaning growth was
277 inhibited by the carbon source; if a well had growth equal to or more than the dextrose well then it was
278 given "+", meaning it was capable of growth on the carbon substrate; finally if the well was in between
279 the negative control and positive control it was given a "V", for variable growth. Nuances of the fungal
280 growth on individual carbon sources required a more gradual scale, and so scores were adjusted to form
281 a range of 1-5 to allow for more accurate average calculation between the three replicates. For this
282 scale: one was no growth or equal to the kits "-", five was the most growth and equivalent to the kit's
283 "+"; numbers in between allowed us to average out the replicates to ensure we had a sliding scale of
284 utilization rather than multiple variable "V" utilizations without a clear idea of how variable the
285 utilization was.

286 *Nitrogen utilization*

287 Nitrogen utilization tests were performed using ten different nitrogen conditions. 100 mM was the
288 concentration used for all compounds that contained one nitrogen atom per molecule: Proline,
289 Ammonium tartrate dibasic, Serine, Sodium Nitrate, Glycine, Glutamate, and Aspartate; 50 mM was the
290 concentration used for Urea because it has two atoms of nitrogen per molecule; 1% w/v of Peptone was
291 used as a positive control; and no nitrogen was added as a condition for a negative control (**Table 2**).
292 Liquid minimal media (MN) with MN salts (not 20x Nitrate salts) was used with the varying nitrogen
293 sources to ensure that no alternative nitrogen source would be available to the fungi. Fungi were first
294 grown up in liquid MEA for 5 days at room temperature to reach maximum density. Then, 1 mL of cells
295 was removed and washed three times with water. 99 µL of each nitrogen source-containing medium
296 was added to six wells in a 96-well plate, for six replicates, and 1 µL of the washed cells was added to
297 each well. 100 µL of each medium was also added to one well each without cells to blank each
298 condition, because the different nitrogen sources created different colors of medium. Daily growth was
299 measured from day 0 to day 7 at 420 nm, using the BioTek Synergy H1 hybrid spectrophotometer.

300 *Optimal growth temperature and range of growth temperatures*

301 To determine the temperature resistance range and optimal growth temperature for each isolate, we
302 grew both fungi at 4 °C, 15 °C, 23 °C (i.e., ambient room temperature), 28 °C, 37 °C, and 42 °C. Isolates
303 were first grown up in 25 mL of MEA for 5 days at room temperature to maximum density. Then 1 mL of
304 cells was removed, and a 10x serial dilution was made from 0x to 100,000x, using pre-filled 1.5mL tubes
305 with 900 µL of MEA and adding 100 µL of the previous tubes each time. Then 5 µL of each serial dilution
306 was spotted onto a square MEA plate which allowed us to determine the carrying capacity of each
307 isolate at the different temperatures. Plates were kept at their respective temperatures for 7 days
308 before observations were made, however the 37 °C and 42 °C incubators required cups of water inside
309 of them to prevent the plates from dehydrating. Plates grown in 42 °C and 37 °C were then allowed to
310 grow at room temp for up to a week to determine if the isolates died at these temperatures or if their
311 growth was just arrested.

312 *UV resistance*

313 Resistance to UV light was observed to determine if these black fungi, with highly melanized cell walls
314 and constant exposure to sunlight in their natural habitat, were in fact UV resistant. To determine this,
315 we used the UVP HL-2000 HybriLinker UV crosslinker as our source of UV light, which has a UV
316 wavelength of 254 nm. Lower wavelengths (100-280 nm) are of the UV-C range, they are considered
317 ionizing radiation and are the most detrimental to living organisms, but are completely blocked by the
318 ozone layer (Molina & Molina, 1986; Schreier et al., 2015). Therefore, using this wavelength we are able
319 to push our organisms beyond the UV limits found in their natural habitat and test extreme amounts of
320 UV exposure. The fungi were inoculated in 25 mL of MEA in a 250 mL Erlenmeyer flask and let grow
321 under shaking conditions at 200 rpm for 5 days at room temperature to reach maximum density. 100 µL
322 of this culture was then spread out onto 6 MEA plates, using a glass spreader. Three plates were kept as
323 the control growth, to compare to the three other plates which were exposed to the UV light.
324 Experimental plates were placed inside of the crosslinker with their lids taken off. Then the plates were
325 exposed to 120 seconds of UV light from a distance of 9.5 cm to the light source at 10,000 $\mu J/cm^2$ (254
326 nm) (Frases et al., 2007). We then wrapped all plates in aluminum foil and placed them in the Percival
327 light incubator set at 23 °C for 2 days. Placing UV-exposed cells in complete dark after exposure is
328 essential for preventing native cell repair mechanisms to act upon any potential mutations, allowing for

329 only those cells that are capable of withstanding the UV exposure without repair mechanisms to grow
330 (Weber, 2005). After 2 days the plates were removed from the aluminum foil and left in the incubator
331 for 5 more days before final observations. To determine whether a particular isolate was resistant to UV
332 exposure, the growth of the isolate exposed to UV was compared to the control growth.

333 *Metal Resistance*

334 Metal resistance is a relatively universal trait in many polyextremotolerant fungal species. Due to the
335 under-studied nature of this particular characteristic in biological soil crusts and fungi, we decided to
336 test if any of our isolates were resistant to any heavy metals which would indicate possible
337 bioremediation capacity. In order to test metal resistance, we used the antibiotic disc method by
338 aliquoting metal solutions onto paper discs and observing zones of clearance. Metals and concentrations
339 used are listed in **Table 3.** For testing, 5 µL of each metal solution was aliquoted onto a dry autoclaved
340 Wattman filter paper disc which was created using a standard hole puncher. These discs were then
341 allowed to air dry and kept at 4 °C for up to a week. Initial growth of the fungal isolates was done in 25
342 mL of MEA, shaking at 200 rpm for 5 days at room temperature. We then spread 100 µL of each fungal
343 isolate onto 100 mm sized MEA plates using a glass spreader to create a lawn. Using flame sterilized
344 tongs our metal paper discs were placed onto the center of the petri dish on top of the fungal lawn and
345 lightly pressed down to ensure the metal disc was touching the plate completely. These plates were
346 then placed in the Percival light incubator at 23 °C with a 12 hr light/dark cycle for up to 2 weeks. Once a
347 zone of clearing was clearly visible amongst the fungal growth (1-2 weeks), the zone of clearing was then
348 measured in cm. Generally, large zones of clearing indicated sensitivity to the metal, whereas zones of
349 reduced size were consisted with resistance to the metal.

350 *Lipid profiles*

351 Comparison of the lipid production of *S. cerevisiae*, *E. dermatitidis*, *E. viscosium*, and *E. limosus* was
352 performed in the presence of fermentable vs. non-fermentable sugars in high and low nitrogen. To test
353 these conditions we grew all four species in four different media types. 1) MEA; 2) MEA + 20 g/L of
354 peptone instead of 2 g/L; 3) MEA with the dextrose replaced with the same weight amount of glycerol;
355 4) MEA with glycerol instead of dextrose and 20 g/L of peptone instead of 2 g/L. All four fungal species
356 were first inoculated in 25 mL of liquid MEA in a 250 mL Erlenmeyer flask and shaken at 200 rpm for 5
357 days at room temperature to reach peak density. Then 100 µL was inoculated into 5 mL of each media in
358 a size 25 mm tube, placed in a roller drum and allowed to grow at room temperature for 5 days.

359 To observe their lipid profile, we performed a standard Bligh Dyer lipid extraction (Bligh & Dyer, 1959).
360 Equal wet weight of each organisms' cells was pelleted and re-suspended in 2 mL of methanol inside of
361 16 mm glass tubes. Tube openings were covered in Durafilm before applying the lid of the tube, then
362 samples were boiled for 5 minutes and let cool for 10 minutes. Then 2 mL of chloroform and 1.6 mL of
363 0.9% NaCl were added, and the tubes were vortexed to fully mix. Tubes were then centrifuged at 5000
364 rpm for 5 minutes to separate the layers. The bottom lipid layer of the suspension was removed and
365 placed in a new glass tube which was then dehydrated using nitrogen gas till the samples became fully
366 dry. Dehydrated samples were then re-suspended with 100 µL of a 9:1 ratio of chloroform : methanol to
367 run the thin layer chromatography (TLC) with. For all samples except the *S. cerevisiae*, 7 µL of the lipid
368 suspension was used to dot the TLC. For *S. cerevisiae,* 10 µL of the lipid suspension was needed. The
369 solvent systems used for TLC were Chloroform : methanol : glacial acetic acid: water 85:12.5:12.5:3 for
370 the Polar lipid solvent system, and Petroleum ether : Diethyl ether : acetic acid 80:20:1 for the neutral

371 lipid solvent system. The TLC plates were loaded with 7 or 10 µL of the re-suspended samples, and they
372 were placed in the Polar solvent system for approximately 30 minutes (half-way up the plate) before
373 transferring to the Neutral Lipid solvent system in a separate container till the solvent front reached just
374 a few cm below the top of the plate. The plate was then removed and dried for 15 minutes, until the
375 solution on the plate was no longer volatile, and the plate was placed in the presence of iodine (Sigma-
376 Aldrich cat. No. 207772) in a glass chamber for 5 minutes until all the lipids were visible. The plates were
377 then immediately placed in plastic covers and scanned and photographed for visualization and
378 documentation.

379 Melanin experiments:

380 *Melanin biosynthesis gene annotation*

381 Melanin biosynthesis in fungi occurs via three different pathways: the DHN pathway which creates
382 allomelanin, the DOPA pathway which creates pheomelanin, and the tyrosine degradation pathway
383 which creates pyomelanin (Cao et al., 2021; Gessler et al., 2014). Most fungal species only contain one
384 melanin biosynthetic pathway, but there are many species in Pezizomycotina, particularly in the genera
385 *Aspergillus* and *Exophiala*, which are capable of producing two or all three forms of melanin (Teixeira et
386 al., 2017). For that reason, we decided to manually annotate the genes involved in all three melanin
387 biosynthetic pathways in *E. viscosium* and *E. limosus* to determine if they too possessed all three
388 melanin biosynthetic pathways. In all cases, the relevant *A. niger* genes were used as queries (Teixeira et
389 al., 2017). Protein sequences for each gene were found using the Aspergillus genome database (AspGD)
390 and were tested using BLAST-P against the filtered model proteins database of *E. viscosium and E.*
391 *limosus* on Mycocosm. Since *A. niger* contains paralogs for some melanin biosynthetic genes, all genes
392 listed in (Teixeira et al., 2017) were used as queries for BLAST searches. Once the melanin biosynthetic
393 genes in *E. viscosium* and *E. limosus* were identified, their highest matching protein sequences were
394 then reverse BLASTed to the *A. niger* genome to determine the reciprocal best hit and ensure true
395 homology.

396 *Regulation of Melanin production using chemical blockers*

397 Once it was established that both isolates contain the potential for production of all three fungal
398 melanins, the effects of known chemical blockers of the DHN and DOPA melanin pathways was used to
399 investigate melanin production. DHN melanin blocker Phthalide and the DOPA melanin blocker Kojic
400 acid were both used in hopes of blocking melanin production in these isolates. Stock solutions were
401 made according to (Pal et al., 2014): Phthalide was diluted in 70% ethanol, and Kojic acid in DMSO.
402 Three separate experiments were performed using these melanin blockers, to determine which method
403 would provide the most informative results.

404 The first was the disc diffusion method whereby Whatman filter paper discs were autoclaved and
405 impregnated with 5 µL of either 10 mM of Phthalide or 10 mg/mL of Kojic acid. Impregnated filter paper
406 discs were then placed on top of freshly spread lawns of either isolates on both MEA and YPD. Lawns
407 were of 50:50 diluted 5-day old cells grown in MEA, and 100 µL of this dilution was spread onto the petri
408 plates with a glass spreader. These plates were then grown at 23 °C with 12 hr light/dark cycles for 5
409 days. Additionally, both a Kojic acid disc and Phthalid discs were placed on fungal lawns ~4 cm apart
410 simultaneously to observe their specific melanin-blocking capabilities on the same cells.

411 Next, we tried adding the melanin blockers directly to the medium as was done in (Pal et al., 2014).
412 Since melanin is more universally distributed in *Exophiala* cells compared to *Aspergillus* cells, we decided
413 to use the highest concentration of both Kojic acid and Phthalide that was used by (Pal et al., 2014),
414 which was 100 mM of each compound. This concentration was added to both solid YPD and MEA after
415 autoclaving, individually and combined. These plates were then used for two forms of growth
416 experiments. Alternatively, we spread a lawn onto YPD and MEA with and without Kojic acid, Phthalide,
417 and both compounds at 100 mM each. Finally, we performed a 10x serial dilution of both *E. viscosium*
418 and *E. limosus* up to 10,000x diluted, and spotted 5 µL of each dilution onto MEA plates with and
419 without Kojic acid, Phthalide, and both compounds. We let both growth experiments grow at 23 °C for 5
420 days with a 12 hr light/dark cycle.

421 *Melanin Extraction and spectrophotometric measurements*

422 Extraction of melanin from a variety of sources has been performed with two main categories of
423 methods: chemical extraction and enzymatic extraction (Pralea et al., 2019). We were unsure which
424 extraction method would be most applicable to these species, so both were performed. The enzymatic
425 extraction method that was used came from (Rosas et al.) (2000). Alternatively, the chemical extraction
426 method, which has been used more extensively in previous works, was derived from (Pal et al., 2014).
427 Their method for extraction and purification of melanin from culture filtrate was adapted and used for
428 all future secreted melanin extractions. Adjustments to the Pal et al. method included: the 6M HCl
429 precipitation took multiple days instead of overnight for melanin to precipitate, then stopping the
430 protocol when 2M NaOH was added to the extracted melanin. We did not continue on to re-
431 precipitation and drying of the melanin as this product did not reprecipitate in any solvents used.

432 Exact methods are as follows. 10 mL of culture was centrifuged at 3,000x g for 5 minutes, and the
433 resulting supernatant was filter sterilized through a 2 µm filter to ensure all cells were removed. The
434 filtered supernatant was then transferred into a 50 mL centrifuge tube, and 40 mL of 6M HCl was added
435 to the tube. The filtrate was then allowed to precipitate out for up to two weeks. Precipitated solutions
436 were then centrifuged at 4000 rpm for 3 minutes, and the resulting supernatant was discarded. The
437 pellet was washed with 2 mL of dd H_2O, vortexed, centrifuged, and the supernatant discarded. Then 3
438 mL of 1:1:1 Chloroform : ethyl acetate : ethanol was added to the samples and vortexed vigorously to
439 ensure as much re-distribution of the melanin was accomplished. The tubes were then centrifuged
440 again, and any resulting clear layers (top and or bottom) were discarded, leaving behind the dark layer. 2
441 mL of water was added to the sample for washing, and the tubes were centrifuged again, and the entire
442 supernatant was discarded. Finally, 1 mL of 2M NaOH was added to each sample to allow for a standard
443 volume added even if the melanin amount and therefore the final volume varied.

444 Extracted melanin samples suspended in 1 mL of 2M NaOH were then diluted 5 µL into 195 µL of 2M
445 NaOH into a 96-well plate, with a 200 µL 2M NaOH blank well. These diluted samples were then read
446 using the BioTek Synergy H1 hybrid spectrophotometer. The settings were for a full spectrum read from
447 230 nm to 700 nm, with 10 nm steps. However, the machine could not read ODs above 4.0, and
448 therefore only data from 300 nm to 700 nm was used.

449 *Melanin secretion and its concentration in the supernatant*

450 To confirm that *E. viscosium* and *E. limosus* are actively secreting melanin, as opposed to dead cells
451 lysing and releasing it, we grew up both species and took daily aliquots for melanin extraction.

452 Additionally, we wanted to compare the melanin secretion capabilities of these species to *E.*
453 *dermatitidis* for a baseline comparison. All three species were grown up in liquid MEA shaking at room
454 temperature for 5 days. Then 2 mL of cells were washed with water three times. 500 µL of washed cells
455 were then inoculated into 100 mL of MEA and YPD in 500 mL flasks. We let the cells grow at 23 °C
456 shaking at 200 rpm for 7 days, removing 11 mL of cells and supernatant daily and pipetting them into 15
457 mL centrifuge tubes. The tubes of cells were then centrifuged at 3000 rpm for 5 minutes, the
458 supernatant was removed, filter sterilized through a 2 µm filter, and placed into a new tube. We filter
459 sterilized the supernatant to ensure that no cells remained in the supernatant, therefore all of the
460 melanin extracted came only from secreted melanin. Melanin was then extracted using the chemical
461 method explained above. Resulting pure melanin for all samples was read with the full spectrum as
462 stated above, and both standard OD and log scale graph were created to confirm the presence of
463 melanin with the proper R^2 value above 0.9 (Pralea et al., 2019).

464 *Increasing amounts of peptone*

465 To assess the role of nitrogen levels in melanin secretion, we initially switched the concentration of
466 peptone added to YPD and MEA media; the new media would be: YPD + 0.2% peptone, and MEA + 2%
467 peptone. We then took both *E. viscosium* and *E. limosus* that was grown in liquid MEA for 5 days shaking
468 at room temperature and plated out the species onto these new media using the same technique as
469 described above for growth comparison on different media. To determine if a more gradual increase in
470 peptone would correlate with a gradual secretion of melanin, we took the base media of MEA (solid)
471 and changed the concentration of peptone to: 0.1%, 0.5%, 1%, 1.5%, 2%, 2.5%, 3%, 3.5%, 4%, and 5%.
472 We then spotted 5 µL of both species onto the plates after performing a 10x serial dilution up to 10,000x
473 dilution. The plates were grown at 23° for 10 days with a 12 hr light/dark cycle.

474 <u>Albino mutant experiments:</u>

475 *Creation of EMS mutants and annotation of their mutations*

476 Genetic modification of these species has not been established yet. However, random mutagenesis via
477 chemical mutagens was performed in the hopes of finding albino mutants, to provide greater insight
478 into the regulation of melanin production. UV exposure which is used frequently as a mutagen for
479 random mutagenesis was attempted, but never resulted in phenotypically distinct mutants or albino
480 mutants. Instead, we used ethyl methyl sulfonate (EMS) to induce G:C to A:T mutations randomly within
481 the genomes of our two species. This was performed using the method by (Winston, 2008). Albino
482 mutants and other interesting pigmentation or morphological mutants were isolated from the resulting
483 mutagenesis, and their DNA was extracted using the same CTAB extraction manner stated above. Their
484 DNA was then sent to the Microbial Genome Sequencing Center (MiGS) for genome re-sequencing and
485 base-called against the wild-type DNA. Resulting mutations were then manually annotated using the JGI
486 Mycocosm genome "search" tool to determine if any genes were disrupted by the mutations to cause
487 the phenotype observed.

488 *Recovery of melanin production in albino mutants*

489 Following recovery of our albino mutant, we attempted to restore melanin production via chemical
490 induction of the other melanin biosynthetic pathways. We did this using hydroxyurea (HU), L-DOPA, and
491 1,8-DHN. Hydroxyurea has been shown to enhance melanin production in *E. dermatitidis*, and L-DOPA is

492 needed for certain fungi to produce melanized structures, including the albino mutant form of *E.*
493 *dermatitidis* WdPKS1 (Dadachova et al., 2007; Paolo et al., 2006; Schultzhaus et al., 2020). Both YPD and
494 MEA medium was made up and 20 mM of HU, 1 mM of L-DOPA, or 1 mM of 1,8-DHN was added to the
495 medium after autoclaving. Our albino mutant was then grown up in the same way as our wild type cells.
496 5 µL of grown cells were spotted onto these media with added compounds and they were grown for 10
497 days at 23 °C 12 hr light/dark cycle.

498 # Results

499 ## Description of *Exophiala viscosium* and *Exophiala limosus*

500 *Exophiala viscosium* CBS 148801 was isolated from Jackman Flats Provincial Park in B.C. Canada. Initial
501 ITS sequencing was performed to obtain potential taxonomic matches. BLAST results to its ITS sequence
502 matched 97.57% to "*Exophiala nigra* strain CBS 535.95" accession number: MH862481.1. Whole
503 genome sequencing and further phylogenetic analyses subsequently revealed that *E. viscosium* is a
504 novel species closely related to *E. sideris* (**Figure 2**).

505 Morphological characterization of *E. viscosium* demonstrated that compared to *E. dermatitidis*, *E.*
506 *viscosium* has much darker pigmentation, and is also a more viscous cell culture. When scraping a colony
507 off the plate it comes up like stretchy tar usually leaving a string of cells hanging off the sterile loop. *E.*
508 *viscosium* does not disperse in water easily when re-suspending, but it does pellet easily at 10,000x g for
509 1 minute. When grown up on a MEA plate for a week or more, it will begin to form a rainbow sheen like
510 an oil slick (**Figure 3A**). Hyphal growth will begin to form into the agar when the plate is left alone at
511 room temperature for more than three weeks. Interestingly, secretion of melanin into the agar can be
512 observed after two weeks on MEA and one week on YPD plates. In liquid culture, this occurs more
513 quickly, with melanin observed in the supernatant starting at 5 days in MEA and 3 days in YPD. The
514 cellular morphology of *E. viscosium* is that of a true yeast. It has large tear-drop shaped cells that usually
515 bud one at a time but can sometimes bud 2-3 times simultaneously (**Figure 3B**). Lipid bodies are
516 frequently observed, as the large circles within cells (**Figure 3B**) and have been confirmed by Nile red
517 staining (data not shown). This isolate grows to its maximum density in 7 days at 23 °C in 25 mL of MEA
518 in a 250 mL Erlenmeyer flask shaken at 200 rpm. *Exophiala viscosium* was originally referred to as
519 "Goopy" due to the nature of its morphology. Accordingly, we have formally named it *Exophiala*
520 *viscosium* for the Latin term of viscous.

521 *Exophiala limosus* CBS 148802 was isolated from a biological soil crust on public land in B.C. Canada. The
522 ITS region of *E. limosus* most strongly matched "*Exophiala nigra* strain CBS 535.95" accession number:
523 MH862481.1 with an identify of 97.67%. Although both *E. viscosium* and *E. limosus* have similar
524 phylogenetic placement, their cellular morphology and budding patterns differ drastically (**Figures 3** &
525 **5**). As seen in **Figure 3D**, the cellular morphology of *E. limosus'* resembles that of *Horatea werneckii* as
526 observed by (Mitchison-Field et al., 2019). Cells are more elongated than *E. viscosium*, and when grown
527 up to maximum density pipetting becomes difficult due to large clumps of cells formed by its more
528 filamentous growth pattern. Both isolates have the consistency of sticky black tar, and an iridescent
529 shine that forms after a week on an MEA plate. *Exophiala limosus* also fails to easily disperse when
530 suspended in water but can be readily pelleted. These observations and the prominence of lipid bodies
531 within the cells (**Figure 3D**) suggests that lipid-derived compounds could cause their sticky, water
532 repelling, iridescent nature. This isolate grows to its maximum density in 7 days at 23 °C in 25 mL of MEA

533 in a 250 mL Erlenmeyer flask shaken at 200 rpm. Originally, *E. limosus* was named "Slimy" to reflect its
534 colony characteristics. Accordingly, we have formally named it *Exophiala limosus* for the Latin term of
535 muddy. Notably, *E. limosus* possesses a looser pellet and is less refractory to re-suspension than *E.*
536 *viscosium*.

537 *Genome description*

538 The genome assembly sizes of these two novel *Exophiala* species are: 28.29 Mbp for *E. viscosium* and
539 28.23 Mbp for *E. limosus* (**Table 4**). These sizes are similar to other yeasts in the genus *Exophiala* and are
540 only a bit smaller than their closest relative *E. sideris* (29.51 Mbp). Although their genomes are smaller
541 than *E. sideris*, predicted gene content is relatively higher; 11344 for *E. viscosium* and 11358 for *E.*
542 *limosus* as compared to 11120 for *E. sideris* (**Table 4**). However, *E. sideris* appears to possess longer
543 genes, transcripts, exons, and introns compared to *E. limosus* and *E. viscosium,* which could also
544 contribute to the gene number to genome size differences (**Table 4**). *E. viscosium* contains the highest
545 GC% amongst the *Exophiala* species listed in **Table 4**. *E. viscosium*'s GC content is even higher than *E.*
546 *limosus* by 2.65%, which given their genetic similarities is quite interesting.

547 *Mating type*

548 *Exophiala* species are one of the many fungal genera whose mating capabilities remain incompletely
549 understood and vary across the genus (Teixeira et al., 2017). The closest species to *E. viscosium* and *E.*
550 *limosus* is *E. sideris,* within which both mating types have been characterized as a single fused gene
551 (Teixeira et al., 2017). Given the known order of genes in regions flanking the MAT locus in *Exophiala*
552 species, we used comparative approaches to determine the mating identities of the sequenced *E.*
553 *viscosium* and *E. limosus* isolates, and to look for possible evidence of homothallism that is also
554 presumed in *E. sideris*. Homologues of the genes *APN2*, *SLA2*, *APC5*, *COX13*, and *MAT1* (*MAT1-1/alpha*)
555 in *E. viscosium* and *E. limosus* were identified via BLAST searches. We found that *APN2* and *SLA2* flank
556 the *MAT* gene of both species, and they also contain the Herpotrichalleaceae-specific mating gene
557 *MAT1-1-4* (**Figure 4**). These results are not surprising, in that this is the exact same order of these genes
558 in *E. sideris*. Interestingly, as Teixeira et al. indicate, in *E. sideris* the *MAT* gene is a fused *MAT1-1/MAT1-*
559 *2* gene with the HMG domain in the middle splitting the α-box in half (Teixeira et al., 2017). When the
560 MAT gene protein sequences of *E. viscosium* and *E. limosus* are aligned with the *MAT* gene of *E. sideris*,
561 we see very high homology indicating that these fungi also contain a fused *MAT* gene. This fused *MAT*
562 gene is theorized to allow these species to be homothallic, although this has not been confirmed
563 experimentally in any of these three species. Additionally, neither *E. viscosium* nor *E. limosus* contain an
564 additional gene between *APN2* and the *MAT1-1-4* that is found in *E. sideris* (Teixeira et al., 2017).
565 Furthermore, *COX13* and *APC5* are about 7,000 bp downstream of the MAT locus in both species, but
566 *COX13* is on the opposite strand in *E. limosus* (**Figure 4**).

567 <u>Phenotyping of *E. viscosium* and *E. limosus*:</u>

568 To further understand the morphology, growth capabilities, and stress responses of *E. viscosium* and *E.*
569 *limosus*, we performed multiple phenotyping experiments. The intent of these experiments was to
570 provide a broader perspective on the potential adaptations that would support the ability of these fungi
571 to successfully colonize biological soil crusts and other extreme niches.

572 *Budding patterns*

573 Due to these species' similarities in colony morphology, observations of budding patterns in these new
574 species became an essential task for differentiation. Microscopy was initially performed on cells grown
575 from solid agar plates, which provided us with basic information that their cell morphology was
576 different, with *E. viscosium* being very round and yeast-shaped and *E. limosus* having more elongated,
577 connected cells. But details regarding their budding patterns and cell polarity we're also needed. Using
578 adapted protocols from (Mitchison-Field et al., 2019) we were able to perform a long-term microscopy
579 time-lapse of the budding patterns of these species using the VALAP (1:1:1 Vasoline: Lanolin: Parafin)
580 method to seal the edges of a coverslip while allowing gas exchange for cells to actively grow (**Figure 6**).
581 From this we were able to observe dramatic differences in the budding types of *E. viscosium* and *E.*
582 *limosus*. *E. viscosium* buds with round cells in initially a distal fashion where the new bud forms 180°
583 from the mother cell origination site, but also forms new buds at a ~90° angle from where the mother
584 bud was formed in a proximal manner (**Figure 5; Video 1**). *E. limosus* on the other hand forms elongated
585 cells in a distal manner, forming longer chains of cells instead of clusters, with axial buds forming at later
586 timepoints (**Figure 5; Video 2**). These morphological differences in budding patterns influences the way
587 these two species grow in a shaking flask. For example, *E. limosus* forms more elongated cells and buds
588 distally which while does not create true hyphae, still creates larger clumps of cells which are not easily
589 pipetted. However, *E. viscosium* since it forms rounder cells and buds with both distal and proximal
590 patterns, does not form extensive clumps in a shaking flask and is more easily pipetted. *E. limosus* also
591 forms more extensive biofilms at the liquid-air interface than *E. viscosium*, likely also due to the
592 elongated cell morphology.

593 *Growth of E. viscosium and E. limosus on 8 different medias:*

594 Growth of *E. viscosium* and *E. limosus* on a variety of different media was done to assess growth
595 requirements and their impact on pigmentation (**Figure 6**). The media used are described in **Table 1**, and
596 include MAG, MEA, MN+NAG, MNV, PDA, Spider, YPD, and V8. The addition of Vitamin mix (Table 1) to
597 any medium, but specifically to MAG and MN, caused the growth of both isolates to become much
598 shinier, blacker (vs. browner), and more yeast-like. Growth on MEA causes the formation of a rainbow
599 sheen, which is not seen on any other medium. Spider medium and YPD caused the formation of a dark-
600 colored halo around colonies of both species. However, the halo around colonies grown on YPD is much
601 darker and extends further than on Spider medium, and *E. viscosium* showed a more extensive halo than
602 *E. limosus*. The ability of both species to grow on V8 medium implies that they can use cellulosic
603 material as a carbon source. Overall, colony growth and pigmentation were similar across of media
604 types for both species (**Figure 6**).

605 *Carbon and nitrogen utilization*

606 Carbon source utilization was determined using Biomerieux C32 carbon strips, which are typically used
607 for identification of human pathogens (Tragiannidis et al., 2012). Following the protocols provided by
608 the vendor, we were able to show that *E. viscosium* and *E. limosus* can utilize a wide range of carbon
609 sources. Triplicates were performed on these strips to ensure results were uniform and representative.
610 Overall, a variety of carbon sources supported robust growth of both species (e.g., D-glucose, L-sorbose,
611 D-galactose, N-acetyl glucosamine, D-sorbitol, D-xylose, glycerol, L-rhamnose, L-arabinose, D-celliobiose,
612 and maltose), and there are only a few quantitative differences in utilization patterns (**Figure 7; Table 5**).
613 Carbon sources that could not support growth include D-rafinose, D-melibiose, methyl-aD-
614 glucopyranoside, and D-lactose. Both species were resistant to cycloheximide and were capable of

615 producing a black color in the presence of esculin ferric citrate (**Figure 7**). Notably, for both *E*. *viscosium*
616 and *E*. *limosus*, growth on some carbon sources, particularly sorbose, levulinic acid, and N-
617 acetyglucosamine, lead to enhanced pigmentation (**Figure 7**).

618 We were particularly interested in patterns of nitrogen utilization for *E*. *viscosium* and *E*. *limosus* given
619 their isolation from a nutrient deplete niche with extensive nitrogen-fixing bacterial populations. Nine
620 different nitrogen sources were tested: five amino acids (aspartate, glutamate, glycine, proline, serine),
621 ammonium tartrate, sodium nitrate, urea, peptone (mixed short chain amino acids) as a positive control,
622 and no nitrogen as a negative control. Both species are incapable of utilizing Aspartate and Glutamate as
623 nitrogen sources (**Figure 8**). Preferred nitrogen sources for both species include ammonia and proline.
624 However, they differ in that *E. viscosium* also prefers urea while *E. limosus* also prefers serine (**Figure 8**).
625 Otherwise, patterns of nitrogen utilization appear generally similar across both species.

626 *Optimal Growth Temperature and Range of growth temperatures*

627 *E*. *viscosium* and *E. limosus* were isolated from an environment that experiences wide seasonal and
628 diurnal temperature changes. As such, we wanted to determine both the optimal growing temperature
629 for these species, as well as the limits at which they are capable of survival. Both isolates were serial
630 diluted and spotted onto MEA plates to determine the carrying capacity at different temperatures. Both
631 *E. viscosium and E. limosus* were capable of growth at 4 °C, 15 °C, 23 °C, and 27 °C, but could not grow at
632 37 °C and 42 °C (**Figure 9**). Optimal growth temperature of both *E. viscosium* and *E. limosus* was 23 °C
633 (**Figure 9**). Growth at 4 °C was slow, but after a year the isolates both species formed extensive colonies
634 and flooded the agar with melanin (**Figure 10**). Although neither species grew at 37 °C, they retained
635 viability as they were able to resume growth following return to 23 °C after three days exposure to 37 °C
636 (**Figure 10**). In contrast, a similar experiment showed that incubation at 42 °C is lethal.

637 *UV and metal resistance*

638 Melanized fungi are recognized for their resistance to UV light, and the possibility of using ionizing
639 radiation as an energy source (Dadachova et al., 2007). To assess the response of *E*. *viscosium* and *E*.
640 *limosus* to UV radiation, they were each exposed to a dose (120 seconds of 10,000 $\mu J/cm^2$ at 254 nm)
641 that was lethal to *S. cerevisiae* and *E. dermatitidis* (data not shown). The same level of exposure did not
642 kill either *E. viscosium* or *E. limosus* (**Figure 11**) but did significantly reduce the number of viable
643 colonies. Strikingly, surviving colonies showed no evidence of induced mutagenesis based on the
644 absence of altered morphologies or pigmentation (**Figure 11**).

645 Polyextremotolerant fungi have been previously noted as having increased metal resistances as a result
646 of their melanized cell wall and other adaptations to harsh environments (Gadd & de Rome, 1988). To
647 test if these two new *Exophiala* spp. possess increased metal resistances when compared to *E.*
648 *dermatitidis* and *S. cerevisiae*, we impregnated Whatman filter discs with various metals of different
649 concentrations. Diameters of zones of clearing revealed no evidence for enhanced metal resistance in *E.*
650 *viscosium* or *E. limosus* (**Table 6**). On the other hand, both species appear to be moderately more
651 sensitive to $NiCl_2$ and $CdCl_2$ (**Table 6**).

652 *Lipid Profiles*

653 Both *E*. *viscosium* and *E*. *limosus* appear to possess abundant lipid bodies (**Figure 3**). This observation
654 along with the unique sticky morphology of both species led us to the idea that they might contain

655 unique or copious amounts of lipids. We performed a Bligh and Dyer lipid extraction followed by thin
656 layer chromatography (TLC) to observe patterns of lipid accumulation in *E. viscosium* and *E. limosus*
657 grown on media that contained fermentable or non-fermentable sugars, both with high nitrogen and
658 low nitrogen. These iterations creating four unique medias would allow us to cover as much of a spread
659 of lipid changes as possible. S. *cerevisiae* and *E. dermatitidis* were also similarly analyzed. Results from
660 this lipid extraction showed that our two new species did not seem to produce any unique or novel
661 amounts or types of lipids when compared to *S. cerevisiae* and *E. dermatitidis* (**Figure 12**).

662 Melanin production and regulation in *E. viscosium* and *E. limosus*

663 *Melanin biosynthesis gene annotation*

664 A defining feature of black yeasts such as *E*. *viscosium* and *E*. *limosus* is their pigmentation caused by the
665 accumulation of melanin (Bell & Wheeler, 1986). Given the presumed importance of melanin to a
666 polyextremotolerant lifestyle, we are interested in understanding how melanin production is regulated
667 in response to environmental inputs. A first step in this process is to determine the types of melanin that
668 *E*. *viscosium* and *E*. *limosus* are capable of producing. To accomplish this, the sequenced genomes of *E.*
669 *viscosium* and *E. limosus* were annotated using protein sequences for all three melanin biosynthetic
670 pathways in *Aspergillus niger* (Teixeira et al., 2017). The list of *A. niger* genes and their homologs in both
671 *E. viscosium* and *E. limosus* are summarized in **Table 7**. Manual annotation and reverse BLASTP of the
672 melanin biosynthesis pathway genes showed that both *E. viscosium* and *E. limosus* have the genetic
673 capability to produce all three forms of known fungal melanins: DOPA melanin (pheomelanin), DHN
674 melanin (allomelanin), and L-tyrosine derived pyomelanin.

675 *Regulation of Melanin production using chemical blockers*

676 Because *E*. *viscosium* and *E*. *limosus* possess the capability to produce all three forms of fungal melanin,
677 we asked whether they were all being produced simultaneously or if one was preferred for production
678 versus secretion. We used chemical blockers for both DOPA melanin and DHN melanin to determine the
679 predominant type of melanin produced on MEA and YPD. Kojic acid blocks the production of DOPA
680 melanin, whereas Phthalide inhibits the synthesis of DHN melanin; both are effective at doses of 1, 10,
681 and 100 µg/mL (Pal et al., 2014).

682 First, we used 100 mM of phthalide and 100 mg/mL of kojic acid in a filter dick assay. Placing drug-
683 impregnated filter discs on freshly spread lawns of cells either individually or with both drugs combined
684 did not block melanin production even though the concentrations of the drugs were higher than that of
685 previous studies (**Figure 13**). Then using Pal et al.'s method of melanin blocking (Pal et al., 2014), we
686 added the highest dosage (100 µg/mL) of Phthalide and Kojic acid individually and combined to agar-
687 solidified MEA, and both spread a lawn of cells and spotted serially diluted cells onto the plates. Neither
688 assay resulted in blockage of melanin production in *E. viscosium* or *E. limosus* (**Figure 13**). However,
689 addition of 100 µg/mL of Phthalide alone did result in their apparent secretion of a dark substance into
690 MEA (**Figure 14**). Overall, chemical inhibition of DOPA melanin or DHN melanin production did not
691 qualitatively reduce colony pigmentation, possibly suggesting that the tyrosine-derived pyomelanin is
692 still being produced.

693 *Melanin Secretion*

694 The appearance of a dark pigment surrounding colonies of *E*. *viscosium* and *E*. *limosus* under specific
695 conditions raised the idea that these yeasts are able to secrete melanin into their local environment. The
696 presence of dark pigments in the supernatants of liquid cultures lent further support to this.

697 Initial studies were performed to determine which media triggered the release of melanin. Both *E.*
698 *viscosium* and *E. limosus* were capable of releasing the most melanin and in the shortest growth time on
699 YPD, with *E. viscosium* seemingly secreting more than *E. limosus* (**Figure 5**). Because YPD and MEA only
700 differ in yeast vs. malt extract as well as the percentage of peptone (2% in YPD, 0.2% in MEA), we first
701 determined if the peptone differences impacted melanin secretion. By switching the peptone amounts
702 in YPD and MEA, we demonstrated that *E. viscosium* acquired the ability to secrete melanin on MEA if it
703 was supplemented with 2% peptone. To extend this observation, we added progressively higher
704 amounts of peptone to MEA media (i.e., 10 different concentrations of peptone ranging from 0.1% to
705 5%). We observed that *E. viscosium* starts secreting melanin on MEA at a peptone amount of 2%, and *E.*
706 *limosus* starts secreting melanin at about 4% peptone (**Figure 16**).

707 *Confirmation of active melanin secretion from living cells*

708 To confirm that the dark pigment in culture supernatants is indeed melanin, we performed a melanin
709 extraction using previously described methods (Pal et al., 2014; Pralea et al., 2019). Although both
710 enzymatic and chemical extraction of melanin was attempted, the chemical extraction process proved
711 to be more efficient at recovering secreted melanin (**Figure 17**). Therefore, all extractions going forward
712 were performed using the chemical extraction method to ensure all melanin was precipitated out of the
713 solution.

714 Growth of *E. viscosium, E. limosus,* and *E. dermatitidis* on YPD and MEA were observed daily for melanin
715 secretion; 11 mL aliquots of their supernatant were removed daily, and the melanin was extracted from
716 each sample. As the experiment progressed, it was obvious that *E. viscosium* and *E. limosus* began
717 secreting melanin on day 3 and secreted more in YPD than in MEA (**Figure 18**). *E. dermatitidis* on the
718 other hand seemed to have a slower build-up of melanin, and melanin wasn't truly obvious in the
719 medium until day 6 in MEA though it can be seen in MEA day 3 in **Figure 18**. Analysis of the optical
720 density (OD) of extracted melanin revealed that melanin amount increased over the course of the
721 experiment, and that greater amounts of melanin are released in YPD for *E. viscosium* and *E. limosus*
722 compared to MEA for *E. dermatitidis* (**Figure 17**). Interestingly, for both *E. viscosium* and *E. limosus*, their
723 peak melanin secretion was on day 6 and not on day 7 (**Figure 19**). There was actually less melanin on
724 day 7 for both species, indicating that the melanin after day 6 was either degrading, or was being taken
725 back up by the cells. This was only obvious with reading the OD results of the extracted melanin, as the
726 supernatants themselves day 5 and on were all strikingly dark and hard to differentiate visually (**Figure**
727 **18**). Extracted melanin from all *E. viscosium* and *E. limosus* samples displayed the typical results from a
728 full spectrum read on pure melanin, *E. dermatitidis* did not show typical melanin spectrum results until
729 day 6 in YPD but were typical every day in MEA. When graphed with OD to Wavelength the sample
730 should have an exponentially decreasing OD as wavelength increases, and when the OD is changed to a
731 log scale, the full spectrum read should be a linear regression with an R^2 value of 0.97 or higher (Pralea
732 et al., 2019). All *E. viscosium* and *E. limosus* samples displayed these features, and therefore we can
733 confirm that the dark nature of their supernatants is caused by actively secreted melanin.

734

735 Genetic analysis of Melanin Production

736 *Recovery of an albino mutant*

737 At this time, molecular tools for the manipulation of *E. viscosium* and *E. limosus* are not yet available.
738 Therefore, we combined classical genetics with genome re-sequencing to initially investigate the
739 regulation of melanin production. Following mutagenesis with the alkylating agent ethyl methyl
740 sulfonate (EMS), mutants following into four distinct phenotypic classes were recovered: pink/albino,
741 crusty, brown, and melanin over-secretion (Data not shown). The most intriguing of these phenotypes
742 was the pink/albino phenotype found in a mutant of *E. limosus* we called EMS 2-11 (**Figure 20**). This
743 mutant is considered albino but colored pink likely due to *Exophiala* spp. production of carotenoids. It
744 has already been shown that blockage of melanin production in *E. dermatitidis* by mutations in *pks1*
745 results in pink instead of white albino colonies because they also produce carotenoids and by-products
746 such as flavolin that are normally masked by melanin (Geis & Szaniszlo, 1984; Geis et al., 1984).

747 Genome re-sequencing of high molecular weight DNA from mutant EMS 2-11 and comparison to the
748 reference *E. limosus* genome revealed a deleterious SNP causing a nonsense mutation in *pks1*. This
749 mutation was on position 2,346,590 in scaffold 3, located in the *pks1* gene, which caused an C -> T
750 mutation on the first position of the codon such that it became a stop codon. Interestingly, *pks1* only
751 functions in one of the three melanin biosynthetic pathways found in *E. limosus*. Only two of the other
752 random mutations found in EMS 2-11 were missense or nonsense mutations. One is a mutation in a
753 transcriptional repressor EZH1, and another is in alcohol dehydrogenase GroES-like/Polyketide synthase
754 enolreductase. Although either of these mutations could contribute to the pink phenotype, it is more
755 likely that a nonsense mutation in *pks1* is solely responsible for the loss of melanin production despite
756 the lack of mutations in the other melanin biosynthetic pathways.

757 *Recovery of melanin production in albino mutant*

758 Pks1 is a polyketide synthase that is essential for the first step in the DHN-melanin/Allomelanin
759 production pathway. To test if "activation" of an alternative melanin production pathway could restore
760 melanin production to the EMS 2-11 mutant, we substituted 1 mM of L-DOPA into the medium. As L-
761 DOPA was shown to recover melanization in a *pks1* deletion mutant of *E. dermatitidis*, thus presumed
762 that it would be taken up by our EMS 2-11 mutant and activate the DOPA melanin/pheomelanin
763 biosynthesis pathway (Dadachova et al., 2007; Paolo et al., 2006). However, substitution of 1 mM L-
764 DOPA into either MEA or YPD did not induce melanin production in the EMS 2-11 *pks1* mutant (**Figure**
765 **20**). These plates were grown in the dark for 10 days, as L-DOPA will auto polymerize into a melanin
766 precursor in the presence of light, and still no melanin production was observed. Hydroxyurea is another
767 compound that in other *Exophiala* species induces melanin production, however addition of 20 mM of
768 Hydroxyurea also did not activate melanin production in our EMS 2-11 albino mutant (**Figure 20**)
769 (Schultzhaus et al., 2020). Finally, we substituted in 1 mM of 1,8-DHN into their media which is the
770 immediate precursor to DHN melanin, in hopes of recovering the expected melanin biosynthetic process
771 with a *pks1* mutant. This did result in recovery of melanized colonies, while on MEA they do not form
772 extensive growth, their cells are still dark, and on YPD active dark colony growth is observed (**Figure 20**).

773

774 Discussion

775 A major limitation to our understanding of the roles played by BSCs in semi-arid ecosystems is our lack
776 of insight into the microbial components of these biofilms and the nature of their functional interactions
777 (Carr et al., 2021). As photoautotrophs, the roles of cyanobacteria and algae in BSCs are clear (Belnap,
778 2002), but the importance of other residents such as fungi and bacteria is less so. Here, we identify two
779 novel species of black yeasts from BSCs; *E. viscosium* and *E. limosus*. In addition to presenting the
780 complete annotated genome sequence for each species, we also provide a relatively detailed profile of
781 their ability to utilize diverse carbon and nitrogen sources, as well as their response to different forms of
782 stress. Most importantly, we demonstrate that *E. viscosium* and *E. limosus* are capable of producing
783 excessive amounts of melanin, including melanin that is secreted at high levels. Our results suggest that
784 by making melanin available as a public good, black yeasts provide a critical service to the broader BSC
785 community.

786 *Description and genome features of E. viscosium and E. limosus*

787 *E. viscosium* and *E. limosus* are two novel fungi from the family Herpotrichielleaceae that we isolated
788 from a lichen-dominated BSC. Distinguishing features of these isolates includes their yeast morphology,
789 pronounced melanization, and production of extracellular material that leads to the formation of
790 "goopy" or "slimy" colonies. Notably, numerous other melanized fungi with filamentous or polymorphic
791 characteristics were isolated from the same BSC communities. These fungi, which will be described in
792 detail elsewhere, grow much more slowly than *E. viscosium* or *E. limosus* and also release much less
793 melanin. Phylogenetic comparisons suggest that the closest relative of *E. viscosium* and *E. limosus* is *E.*
794 *sideris*. Comparison of their respective annotated genome sequences revealed that overall gene content
795 and characteristics are similar across all three species. *E. sideris* belongs to the *jeanselmei*-clade of
796 *Exophiala* species; it is typically recovered from highly polluted environments and is not known to be
797 pathogenic (Seyedmousavi et al., 2011). The failure of *E. viscosium* and *E. limosus* to grow at 37 ^{o}C
798 reinforces the point that species within this clade are less likely to possess the capacity of causing
799 disease in mammals. One interesting feature that the genome comparisons of *E. sideris* to *E. viscosium*
800 and *E. limosus* revealed was that *E. sideris* contains a lower predicted gene content than the other two
801 isolates. This could be a factor of their differences in their ecology and lifestyles. *E. sideris* was isolated
802 from a highly toxic environment containing arsenate, hydrocarbons, and other toxins meaning this
803 species had to specialize in withstanding these toxins rather than generalizing its survival genetic
804 toolbox (Seyedmousavi et al., 2011). MAT organization of the MAT locus between these homothallic
805 species is very similar, all containing a fused *MAT* gene, with the exception of different transcript
806 directionality for the flanking *cox13* and *apc5* genes. Many *Exophiala* species are indicated to be
807 heterothallic, even closely related species to *E. sideris* such as *E. oligosperma* and *E. spinifera* are
808 heterothallic (Teixeira et al., 2017; Untereiner & Naveau, 1999). Whereas *E. sideris* itself and now *E.*
809 *viscosium* and *E. limosus* all contain a fused or cryptic MAT gene which has been hypothesized to cause
810 homothallism as a result of a parasexual cycle that occurred (Teixeira et al., 2017). Further investigation
811 of these ideas will require demonstration that these *Exophiala* species undergo sexual development.

812 *Phenotypic characterization of E. viscosium and E. limosus*

813 Our results show that *E. viscosium* and *E. limosus* are capable of using a diverse array of carbon sources.
814 These include mannitol, ribitol, and glucose, which are considered the main carbon sources exchanged
815 between photobionts and their mycobiont partners in lichens (Richardson et al., 1967; Yoshino et al.,
816 2020). Although, *E. viscosium* and *E. limosus* are able to use most nitrogen sources provided, glutamate

817 and aspartate are clearly not being taken up or used, unlike in yeasts such as *S. cerevisiae* where
818 glutamate is a more favorable nitrogen source used for multiple core metabolism and amino acid
819 production processes (Ljungdahl & Daignan-Fornier, 2012). Because peptone is a favorable nitrogen
820 source for *E. viscosium* and *E. limosus*, it is likely that these species can import peptides and degrade
821 them as sources of ammonia. Their preferred nitrogen source is ammonium/ammonia though, which in
822 their ecological environment would likely be produced by cyanobacteria and other nitrogen-fixing
823 bacteria (Belnap, 2002). However, they can also use nitrate and urea as nitrogen sources, again pointing
824 to their metabolic flexibility in their nutrient deplete ecosystem.

825 A characteristic feature of BSCs is the inherently stressful nature of these ecosystems. Of note, *E*.
826 *viscosium* and *E. limosus* were isolated from a site that can experience extremes in temperature, UV
827 exposure, and soil wetness/osmotic pressure. Although the optimal growth range for these species is
828 from 15 °C to 27 °C, they are capable of slow growth at 4 °C and while they do not grow at 37 °C, they do
829 remain viable after 72 consecutive hours of exposure to this temperature. The ability to grow at 4°C,
830 albeit slowly, presumably contributes to the success of fungi such *E*. *viscosium* and *E. limosus* in adapting
831 to BSCs in colder drylands. A broader comparison of microbiomes and associated functional traits
832 between cold-adapted BSCs and those found in hot deserts would be an informative approach to
833 identifying microbial species and/or physiological factors that underlie temperature adaptation.

834 As for resistance to UV radiation, *E. viscosium* and *E. limosus* were both able to survive the high
835 exposure of UV-C that was used and were uniquely resistant to standard UV mutagenesis conditions.
836 Potential mechanisms that might contribute to UV resistance include the presence of melanin or other
837 defensive compounds, some of which could be public goods provided by other constituents of the BSC
838 community, or an enhanced capacity to repair damaged DNA. This will ultimately be an interesting topic
839 to investigate in the future.

840 One feature we expected to find in *E. viscosium* and *E. limosus* but we did not necessarily observe was
841 higher metal resistance. Melanin is known to enhance resistances to metals (Bell & Wheeler, 1986;
842 Gadd, 1994; Gorbushina, 2007; Purvis et al., 2004), and so we predicted that these species would have
843 increased metal tolerance when compared to non-melanized fungi. However, of the metals tested, only
844 $AgNO_3$ and $CuCl_2$ showed a decreased zone of clearing in *E. viscosium* and *E. limosus*, compared to *S.*
845 *cerevisiae* and *E. dermatitidis*. A potential explanation for the latter observation is that melanin has a
846 higher affinity for copper due to the phenolic compounds within the polymer (Gadd & de Rome, 1988).

847 *Secretion of melanin by E. viscosium and E. limosus*

848 Melanin is considered an expensive secondary metabolite to produce because it is made up of
849 conglomerates of polyphenols and as such contains many carbons (Schroeder et al., 2020). Therefore, it
850 would be assumed that an organism would not want to create melanin just to export it out of the cell
851 unless there was a beneficial reason behind it. Additionally, there are not many fungi known to secrete
852 melanin and few in the genus *Exophiala*, so the possibility of novel species that secrete melanin into
853 their surroundings was intriguing. Both novel fungi have the genetic makeup to produce all three types
854 of fungal melanin: allomelanin (DHN derived), pyomelanin (L-tyrosine derived), and pheomelanin (L-
855 DOPA derived); but it is still unknown how these melanin biosynthetic pathways are regulated, and
856 which are being actively produced.

857 In our attempts to understand the regulation of melanin production by *E. viscosium* and *E. limosus* we
858 tried blocking individual pathways using known chemical blockers of DHN and DOPA melanin, phthalide
859 and kojic acid respectively. Neither blocker, nor their combination at the highest amounts used were
860 able to block the production of melanin in either species. If these species have the capability to produce
861 all three melanins, then it is possible that they are producing more than one at the same time. This
862 could be the case here, since the combination of both kojic acid and phthalide still resulted in melanized
863 cells which would indicate that tyrosine-derived pyomelanin was the cause of melanization.

864 Linked regulation of potentially multiple forms of melanin was observed with our EMS-induced mutant
865 in which the *pks1* gene contained a nonsense mutation. Although *pks1* is the first enzyme involved in
866 only the production of DHN-derived allomelanin, the cells that resulted from this mutation were albino.
867 Theoretically, these cells should have still been capable of producing the two other melanins as their
868 pathways were seemingly not disrupted by any mutations, but this was not the case. Addition of L-DOPA
869 has been shown to induce melanization in a *pks1* deletion mutant of *E. dermatitidis* (Paolo et al., 2006),
870 which would indicate that it is capable of producing both pheomelanin and allomelanin. However, the
871 same experiment performed on *E. limosus*' *pks1* nonsense mutant did not recover melanization.
872 Therefore, it is possible that; (i) *E. viscosium* and *E. limosus* only produce DHN-derived allomelanin and
873 disruption of *pks1* causes all melanin production to shut down, (ii) *pks1* (or downstream creation of
874 allomelanin) is essential for the regulation of other melanin productions, or (iii) pheomelanin and
875 pyomelanin are only produced under specific conditions that were not used during analysis of the
876 mutants.

877 Our experiments also showed that *E. viscosium* and *E. limosus* actively secrete melanin when they are
878 viable and growing. We observed that melanin began to accumulate starting as early as day 2, therefore
879 suggesting live cells are secreting melanin and not leaked from dead lysed cells. We also observed a
880 decrease in melanin concentrations after day 6 in both YPD and MEA, which raises the intriguing
881 potential for melanin uptake or degradation by *E. viscosium* and *E. limosus*.

882 The medium that stimulated the most melanin secretion is YPD which has 10x more nitrogen (2% vs.
883 0.2%) than the alternative medium we use, MEA, which neither fungus secrete melanin into when
884 plated on solid media. This led us to believe that nitrogen amount could potentially have an effect on
885 the production of secreted melanin, which we did observe as we increased peptone amounts in the
886 medium. Interestingly, the only fungal melanin that has nitrogen in its precursor structure is the DOPA
887 derived pheomelanin. This was one of two melanins that could be produced in the presence of
888 phthalide, which we observed also induced the secretion of melanin in these fungi. This provides
889 support that the secreted melanin is either pheomelanin, as it requires more nitrogen in order to be
890 produced, or that the production of pheomelanin (DOPA) and the water soluble pyomelanin (Turick et
891 al., 2010) are linked.

892 *Insights into the niche of polyextremotolerant fungi within the biological soil crust consortium*

893 Fungal residents of BSC communities include lichenized mycobionts, lichenicolous fungi, endolichenic
894 fungi, and free-living fungi. Although the latter are likely not directly associated with lichens themselves,
895 they are surrounded by algae, cyanobacteria, and other bacteria in the same way that lichen-associated
896 fungi are surrounded by a similar community of microbes. This raises the intriguing possibility that fungi
897 such as *E. viscosium* and *E. limosus* might transiently associated with phototrophs in response to specific
898 environmental conditions. Members of the genus *Exophiala* (Class Eurotiomycetes) are phylogenetically

899 related to the lichen-forming Verrucariales, and reside between Lecanoromycetes and Lichinomycetes
900 (James et al., 2006). Additionally, lifestyle changes within Eurotiomycetes contributed to the
901 polyphyletic nature of lichenization within the Ascomycetes, but since surrounding taxa are lichenized it
902 is more likely that these species lost lichenization than three distinct lichenization events occurring
903 within closely related species (Lutzoni et al., 2001). Because *E. viscosium* and *E. limosus* have lichenized
904 ancestors, they could conceivably have lost their "true lichenization" capabilities, but maintained the
905 genetic tools to interact with algae, cyanobacteria, and other bacteria to form lichen-like symbioses. As
906 these are two newly identified species, more extensive ecological and molecular investigation is needed
907 to determine the extent to which these taxa are found in BSCs and to elucidate their species interaction
908 networks.

909 Correlation between environmental nitrogen availability and secreted melanin amounts could have
910 strong implications for interactions between these fungi found in BSCs and their nitrogen-fixing
911 community partners. The presumed source of nitrogen used to enhance the secretion of melanin would
912 be from nitrogen-fixing prokaryotes such as cyanobacteria, other bacteria, and archaea in the
913 community. Our results suggest that the availability of these nitrogen-fixers to provide fungal cells with
914 ammonia could subsequently induce the secretion of melanin that then provides protective services to
915 the broader BSC community. Secreted melanin could function at the community-level to maintain
916 respiration and growth under varying temperature conditions while also mitigating the effects of
917 desiccation and exposure to UV, extending the window of time allotted for optimal photosynthetic
918 capabilities (Carr et al., 2021; Honegger, 1997; Honegger & Haisch, 2001; Lange & Tenhunen, 1981;
919 Nybakken et al., 2004). Moreover, the secreted melanin could simultaneously serve as an external
920 source of carbon used by the fungi and possibly others when the environment does not allow for
921 photosynthesis. In either scenario, the seemingly wasteful secretion of melanin by *E. viscosium* and *E.*
922 *limosus* instead represents the optimal sharing of an expensive public good for the overall betterment of
923 the BSC community in which they reside.

924 The availability of complete, annotated genome sequences for *E*. *viscosium* and *E. limosus* will enable
925 more detailed investigations of the mechanisms that support the adaptation of these fungi to extreme
926 environments. This in turn should provide greater insight into the roles that these fungi play in the BSC
927 community. Of particular interest will be the regulatory mechanisms that coordinate the production of
928 different types of melanin in response to environmental and chemical inputs. Moreover, the broad
929 applicability of melanin as a bioproduct has triggered growing interest in microorganisms that secrete
930 this polymer. In this context, *E*. *viscosium* and *E. limosus* could potentially serve as excellent platforms
931 for additional engineering focused on optimizing or tailoring the type of melanin produced in responses
932 to specific applications.

933

934 <u>Acknowledgements</u>

935 The authors would like to acknowledge Dr. Rajib Saha for providing a pre-print review of this work, with
936 his guidance we were able to make this manuscript as clear and concise as possible. The work (proposal:
937 10.46936/10.25585/60001081) conducted by the U.S. Department of Energy Joint Genome Institute, a
938 DOE Office of Science User Facility, is supported by the Office of Science of the U.S. Department of
939 Energy under Contract No. DE-AC02-05CH11231. Funding for this work was provided by NASA grant
940 number 80NSSC17K0737.

Citations:

Ametrano, C. G., Selbmann, L., & Muggia, L. (2017). A standardized approach for co-culturing Dothidealean rock-inhabiting fungi and lichen photobionts in vitro. *Symbiosis*, *73*(1), 35-44.

Bates, S. T., Garcia-Pichel, F., & Nash III, T. (2010). Fungal components of biological soil crusts: insights from culture-dependent and culture-independent studies. *Bibliotheca Lichenologica*, *105*, 197-210.

Bates, S. T., Reddy, G. S., & Garcia-Pichel, F. (2006). Exophiala crusticola anam. nov.(affinity Herpotrichiellaceae), a novel black yeast from biological soil crusts in the Western United States. *International journal of systematic and evolutionary microbiology*, *56*(11), 2697-2702.

Bell, A. A., & Wheeler, M. H. (1986). Biosynthesis and functions of fungal melanins. *Annual review of phytopathology*, *24*(1), 411-451.

Belnap, J. (2002). Nitrogen fixation in biological soil crusts from southeast Utah, USA. *Biology and fertility of soils*, *35*(2), 128-135.

Belnap, J. (2003). The world at your feet: desert biological soil crusts. *Frontiers in Ecology and the Environment*, *1*(4), 181-189.

Belnap, J., Büdel, B., & Lange, O. L. (2001). Biological soil crusts: characteristics and distribution. In *Biological soil crusts: structure, function, and management* (pp. 3-30). Springer.

Belnap, J., & Eldridge, D. (2001). Disturbance and recovery of biological soil crusts. In *Biological soil crusts: structure, function, and management* (pp. 363-383). Springer.

Belnap, J., & Lange, O. L. (2003). *Biological soil crusts: structure, function, and management* (Vol. 150). Springer.

Bligh, E. G., & Dyer, W. J. (1959). A rapid method of total lipid extraction and purification. *Canadian journal of biochemistry and physiology*, *37*(8), 911-917.

Bowker, M. A., Reed, S., Belnap, J., & Phillips, S. (2002). Temporal variation in community composition, pigmentation, and Fv/Fm of desert cyanobacterial soil crusts. *Microbial Ecology*, 13-25.

Bowker, M. A., Soliveres, S., & Maestre, F. T. (2010). Competition increases with abiotic stress and regulates the diversity of biological soil crusts. *Journal of Ecology*, *98*(3), 551-560.

Cao, W., Zhou, X., McCallum, N. C., Hu, Z., Ni, Q. Z., Kapoor, U., . . . Mantanona, A. J. (2021). Unraveling the structure and function of melanin through synthesis. *Journal of the American Chemical Society*, *143*(7), 2622-2637.

Carr, E. C., Harris, S. D., Herr, J. R., & Riekhof, W. R. (2021). Lichens and biofilms: Common collective growth imparts similar developmental strategies. *Algal Research*, *54*, 102217.

Castresana, J. (2000). Selection of conserved blocks from multiple alignments for their use in phylogenetic analysis. *Molecular biology and evolution*, *17*(4), 540-552.

976 Cordero, R. J., & Casadevall, A. (2017). Functions of fungal melanin beyond virulence. *Fungal Biology*
977 *Reviews*, *31*(2), 99-112.

978 Cubero, O. F., Crespo, A., Fatehi, J., & Bridge, P. D. (1999). DNA extraction and PCR amplification method
979 suitable for fresh, herbarium-stored, lichenized, and other fungi. *Plant Systematics and*
980 *Evolution*, *216*(3), 243-249.

981 Dadachova, E., Bryan, R. A., Huang, X., Moadel, T., Schweitzer, A. D., Aisen, P., . . . Casadevall, A. (2007).
982 Ionizing radiation changes the electronic properties of melanin and enhances the growth of
983 melanized fungi. *PloS one*, *2*(5), e457.

984 De Hoog, G., Vicente, V., Caligiorne, R., Kantarcioglu, S., Tintelnot, K., Gerrits van den Ende, A., & Haase,
985 G. (2003). Species diversity and polymorphism in the Exophiala spinifera clade containing
986 opportunistic black yeast-like fungi. *Journal of Clinical Microbiology*, *41*(10), 4767-4778.

987 Donlan, R. M., & Costerton, J. W. (2002). Biofilms: survival mechanisms of clinically relevant
988 microorganisms. *Clinical microbiology reviews*, *15*(2), 167-193.

989 Frases, S., Salazar, A., Dadachova, E., & Casadevall, A. (2007). Cryptococcus neoformans can utilize the
990 bacterial melanin precursor homogentisic acid for fungal melanogenesis. *Applied and*
991 *environmental microbiology*, *73*(2), 615-621.

992 Gadd, G. M. (1994). Interactions of fungi with toxic metals. *The Genus Aspergillus*, 361-374.

993 Gadd, G. M., & de Rome, L. (1988). Biosorption of copper by fungal melanin. *Applied microbiology and*
994 *biotechnology*, *29*(6), 610-617.

995 Geis, P. A., & Szaniszlo, P. J. (1984). Carotenoid pigments of the dematiaceous fungus Wangiella
996 dermatitidis. *Mycologia*, *76*(2), 268-273.

997 Geis, P. A., Wheeler, M. H., & Szaniszlo, P. J. (1984). Pentaketide metabolites of melanin synthesis in the
998 dematiaceous fungus Wangiella dermatitidis. *Archives of microbiology*, *137*(4), 324-328.

999 Gessler, N., Egorova, A., & Belozerskaya, T. (2014). Melanin pigments of fungi under extreme
1000 environmental conditions. *Applied Biochemistry and Microbiology*, *50*(2), 105-113.

1001 Gnerre, S., MacCallum, I., Przybylski, D., Ribeiro, F. J., Burton, J. N., Walker, B. J., . . . Jaffe, D. B. (2011).
1002 High-quality draft assemblies of mammalian genomes from massively parallel sequence data.
1003 *Proceedings of the National Academy of Sciences*, *108*(4), 1513-1518.
1004 https://doi.org/10.1073/pnas.1017351108

1005 Gorbushina, A. A. (2007). Life on the rocks. *Environmental microbiology*, *9*(7), 1613-1631.

1006 Gostinčar, C., Grube, M., De Hoog, S., Zalar, P., & Gunde-Cimerman, N. (2009). Extremotolerance in
1007 fungi: evolution on the edge. *FEMS microbiology ecology*, *71*(1), 2-11.

1008 Gostinčar, C., Grube, M., & Gunde-Cimerman, N. (2011). Evolution of fungal pathogens in domestic
1009 environments? *Fungal biology*, *115*(10), 1008-1018.

1010 Gostinčar, C., Muggia, L., & Grube, M. (2012). Polyextremotolerant black fungi: oligotrophism, adaptive
1011 potential, and a link to lichen symbioses. *Frontiers in Microbiology*, *3*, 390.

1012 Grabherr, M. G., Haas, B. J., Yassour, M., Levin, J. Z., Thompson, D. A., Amit, I., . . . Zeng, Q. (2011). Full-
1013 length transcriptome assembly from RNA-Seq data without a reference genome. *Nature*
1014 *biotechnology*, *29*(7), 644-652.

1015 Grigoriev, I. V., Nikitin, R., Haridas, S., Kuo, A., Ohm, R., Otillar, R., . . . Shabalov, I. (2013). MycoCosm
1016 portal: gearing up for 1000 fungal genomes. *Nucleic Acids Research*, *42*(D1), D699-D704.
1017 https://doi.org/10.1093/nar/gkt1183

1018 Grube, M., Cernava, T., Soh, J., Fuchs, S., Aschenbrenner, I., Lassek, C., . . . Sensen, C. W. (2015).
1019 Exploring functional contexts of symbiotic sustain within lichen-associated bacteria by
1020 comparative omics. *The ISME journal*, *9*(2), 412-424.

1021 Hom, E. F., & Murray, A. W. (2014). Niche engineering demonstrates a latent capacity for fungal-algal
1022 mutualism. *Science*, *345*(6192), 94-98.

1023 Honegger, R. (1997). Metabolic interactions at the mycobiont-photobiont interface in lichens. In *Plant*
1024 *relationships* (pp. 209-221). Springer.

1025 Honegger, R., & Haisch, A. (2001). Immunocytochemical location of the (1→ 3)(1→ 4)-β-glucan lichenin
1026 in the lichen-forming ascomycete Cetraria islandica (Icelandic moss). *New phytologist*, *150*(3),
1027 739-746.

1028 James, T. Y., Kauff, F., Schoch, C. L., Matheny, P. B., Hofstetter, V., Cox, C. J., . . . Miadlikowska, J. (2006).
1029 Reconstructing the early evolution of Fungi using a six-gene phylogeny. *Nature*, *443*(7113), 818-
1030 822.

1031 Katoh, K., Misawa, K., Kuma, K. i., & Miyata, T. (2002). MAFFT: a novel method for rapid multiple
1032 sequence alignment based on fast Fourier transform. *Nucleic acids research*, *30*(14), 3059-3066.

1033 Kobayashi, N., Muramatsu, T., Yamashina, Y., Shirai, T., Ohnishi, T., & Mori, T. (1993). Melanin reduces
1034 ultraviolet-induced DNA damage formation and killing rate in cultured human melanoma cells.
1035 *Journal of investigative dermatology*, *101*(5), 685-689.

1036 Kuo, A., Bushnell, B., & Grigoriev, I. V. (2014). Fungal genomics: sequencing and annotation. *Advances in*
1037 *Botanical Research*, *70*, 1-52.

1038 Lan, S., Wu, L., Zhang, D., & Hu, C. (2012). Successional stages of biological soil crusts and their
1039 microstructure variability in Shapotou region (China). *Environmental Earth Sciences*, *65*(1), 77-
1040 88.

1041 Lange, O., & Tenhunen, J. (1981). Moisture content and CO2 exchange of lichens. II. Depression of net
1042 photosynthesis in Ramalina maciformis at high water content is caused by increased thallus
1043 carbon dioxide diffusion resistance. *Oecologia*, *51*(3), 426-429.

1044 Letunic, I., & Bork, P. (2021). Interactive Tree Of Life (iTOL) v5: an online tool for phylogenetic tree
1045 display and annotation. *Nucleic acids research*, *49*(W1), W293-W296.

1046 Ljungdahl, P. O., & Daignan-Fornier, B. (2012). Regulation of amino acid, nucleotide, and phosphate
1047 metabolism in Saccharomyces cerevisiae. *Genetics*, *190*(3), 885-929.

1048 Lutzoni, F., Pagel, M., & Reeb, V. (2001). Major fungal lineages are derived from lichen symbiotic
1049 ancestors. *Nature*, *411*(6840), 937-940.

1050 Maier, S., Muggia, L., Kuske, C. R., & Grube, M. (2016). Bacteria and non-lichenized fungi within
1051 biological soil crusts. In *Biological Soil Crusts: An Organizing Principle in Drylands* (pp. 81-100).
1052 Springer.

1053 McFarland, J. (1907). The nephelometer: an instrument for estimating the number of bacteria in
1054 suspensions used for calculating the opsonic index and for vaccines. *Journal of the American*
1055 *Medical Association*, *49*(14), 1176-1178.

1056 Mitchison-Field, L. M. Y., Vargas-Muñiz, J. M., Stormo, B. M., Vogt, E. J. D., Van Dierdonck, S., Pelletier, J.
1057 F., . . . Gladfelter, A. S. (2019). Unconventional Cell Division Cycles from Marine-Derived Yeasts.
1058 *Current Biology*, *29*(20), 3439-3456.e3435. https://doi.org/10.1016/j.cub.2019.08.050

1059 Molina, L., & Molina, M. (1986). Absolute absorption cross sections of ozone in the 185-to 350-nm
1060 wavelength range. *Journal of Geophysical Research: Atmospheres*, *91*(D13), 14501-14508.

1061 Nybakken, L., Solhaug, K. A., Bilger, W., & Gauslaa, Y. (2004). The lichens Xanthoria elegans and Cetraria
1062 islandica maintain a high protection against UV-B radiation in Arctic habitats. *Oecologia*, *140*(2),
1063 211-216.

1064 Pal, A. K., Gajjar, D. U., & Vasavada, A. R. (2014). DOPA and DHN pathway orchestrate melanin synthesis
1065 in Aspergillus species. *Medical mycology*, *52*(1), 10-18.

1066 Paolo, W. F., Dadachova, E., Mandal, P., Casadevall, A., Szaniszlo, P. J., & Nosanchuk, J. D. (2006). Effects
1067 of disrupting the polyketide synthase gene WdPKS1 in Wangiella [Exophiala] dermatitidis on
1068 melanin production and resistance to killing by antifungal compounds, enzymatic degradation,
1069 and extremes in temperature. *BMC microbiology*, *6*(1), 1-16.

1070 Perez-Cuesta, U., Aparicio-Fernandez, L., Guruceaga, X., Martin-Souto, L., Abad-Diaz-de-Cerio, A.,
1071 Antoran, A., . . . Rementeria, A. (2020). Melanin and pyomelanin in Aspergillus fumigatus: from
1072 its genetics to host interaction. *International Microbiology*, *23*(1), 55-63.

1073 Pralea, I.-E., Moldovan, R.-C., Petrache, A.-M., Ilieș, M., Hegheș, S.-C., Ielciu, I., . . . Radu, M. (2019). From
1074 extraction to advanced analytical methods: The challenges of melanin analysis. *International*
1075 *journal of molecular sciences*, *20*(16), 3943.

1076 Price, M. N., Dehal, P. S., & Arkin, A. P. (2009). FastTree: computing large minimum evolution trees with
1077 profiles instead of a distance matrix. *Molecular biology and evolution*, *26*(7), 1641-1650.

1078 Purvis, O. W., Bailey, E. H., McLean, J., Kasama, T., & Williamson, B. J. (2004). Uranium biosorption by
1079 the lichen Trapelia involuta at a uranium mine. *Geomicrobiology Journal*, *21*(3), 159-167.

1080 Pócs, T. (2009). Cyanobacterial crust types, as strategies for survival in extreme habitats. *Acta Botanica*
1081 *Hungarica*, *51*(1-2), 147-178.

1082 Płonka, P., & Grabacka, M. (2006). Melanin synthesis in microorganisms: biotechnological and medical
1083 aspects. *Acta Biochimica Polonica*, *53*(3).

1084 Rajeev, L., Da Rocha, U. N., Klitgord, N., Luning, E. G., Fortney, J., Axen, S. D., . . . Kerfeld, C. A. (2013).
1085 Dynamic cyanobacterial response to hydration and dehydration in a desert biological soil crust.
1086 *The ISME journal*, *7*(11), 2178-2191.

1087 Richardson, D., Smith, D., & Lewis, D. (1967). Carbohydrate movement between the symbionts of
1088 lichens. *Nature*, *214*(5091), 879-882.

1089 Rosas, Á. L., Nosanchuk, J. D., Gómez, B. L., Edens, W. A., Henson, J. M., & Casadevall, A. (2000). Isolation
1090 and serological analyses of fungal melanins. *Journal of immunological methods*, *244*(1-2), 69-80.

1091 Schreier, W. J., Gilch, P., & Zinth, W. (2015). Early events of DNA photodamage. *Annual review of*
1092 *physical chemistry*, *66*, 497-519.

1093 Schroeder, W. L., Harris, S. D., & Saha, R. (2020). Computation-driven analysis of model polyextremo-
1094 tolerant fungus exophiala dermatitidis: defensive pigment metabolic costs and human
1095 applications. *IScience*, *23*(4), 100980.

1096 Schultzhaus, Z., Romsdahl, J., Chen, A., Tschirhart, T., Kim, S., Leary, D., & Wang, Z. (2020). The response
1097 of the melanized yeast Exophiala dermatitidis to gamma radiation exposure. *Environmental*
1098 *microbiology*, *22*(4), 1310-1326.

1099 Seyedmousavi, S., Badali, H., Chlebicki, A., Zhao, J., Prenafeta-Boldu, F. X., & De Hoog, G. S. (2011).
1100 Exophiala sideris, a novel black yeast isolated from environments polluted with toxic alkyl
1101 benzenes and arsenic. *Fungal biology*, *115*(10), 1030-1037.

1102 Teixeira, M. d. M., Moreno, L. F., Stielow, B., Muszewska, A., Hainaut, M., Gonzaga, L., . . . Souza, R.
1103 (2017). Exploring the genomic diversity of black yeasts and relatives (Chaetothyriales,
1104 Ascomycota). *Studies in mycology*, *86*, 1-28.

1105 Tragiannidis, A., Fegeler, W., Rellensmann, G., Debus, V., Müller, V., Hoernig-Franz, I., . . . Groll, A.
1106 (2012). Candidaemia in a European Paediatric University Hospital: a 10-year observational study.
1107 *Clinical Microbiology and Infection*, *18*(2), E27-E30.

1108 Turick, C. E., Knox, A. S., Becnel, J. M., Ekechukwu, A. A., & Milliken, C. E. (2010). Properties and function
1109 of pyomelanin. *Biopolymers*, *449*, 72.

1110 Untereiner, W. A., & Naveau, F. A. (1999). Molecular systematics of the Herpotrichiellaceae with an
1111 assessment of the phylogenetic positions of Exophiala dermatitidis and Phialophora americana.
1112 *Mycologia*, *91*(1), 67-83.

1113 Weber, S. (2005). Light-driven enzymatic catalysis of DNA repair: a review of recent biophysical studies
1114 on photolyase. *Biochimica et Biophysica Acta (BBA)-Bioenergetics*, *1707*(1), 1-23.

1115 White, T. J., Bruns, T., Lee, S., & Taylor, J. (1990). 38 - AMPLIFICATION AND DIRECT SEQUENCING OF
1116 FUNGAL RIBOSOMAL RNA GENES FOR PHYLOGENETICS. In M. A. Innis, D. H. Gelfand, J. J.
1117 Sninsky, & T. J. White (Eds.), *PCR Protocols* (pp. 315-322). Academic Press.
1118 https://doi.org/https://doi.org/10.1016/B978-0-12-372180-8.50042-1

1119 Winston, F. (2008). EMS and UV mutagenesis in yeast. *Current protocols in molecular biology*, *82*(1),
1120 13.13 B. 11-13.13 B. 15.

1121 Yoshino, K., Yamamoto, K., Masumoto, H., Degawa, Y., Yoshikawa, H., Harada, H., & Sakamoto, K. (2020).
1122 Polyol-assimilation capacities of lichen-inhabiting fungi. *The Lichenologist*, *52*(1), 49-59.

1123 Zanne, A. E., Abarenkov, K., Afkhami, M. E., Aguilar-Trigueros, C. A., Bates, S., Bhatnagar, J. M., . . .
1124 Crowther, T. W. (2020). Fungal functional ecology: bringing a trait-based approach to plant-
1125 associated fungi. *Biological Reviews*, *95*(2), 409-433.

1126 Zerbino, D. R., & Birney, E. (2008). Velvet: algorithms for de novo short read assembly using de Bruijn
1127 graphs. *Genome research*, *18*(5), 821-829.

1128 Zupančič, J., Novak Babič, M., Zalar, P., & Gunde-Cimerman, N. (2016). The black yeast Exophiala
1129 dermatitidis and other selected opportunistic human fungal pathogens spread from dishwashers
1130 to kitchens. *PLoS One*, *11*(2), e0148166.

1131

1132

1133

1134

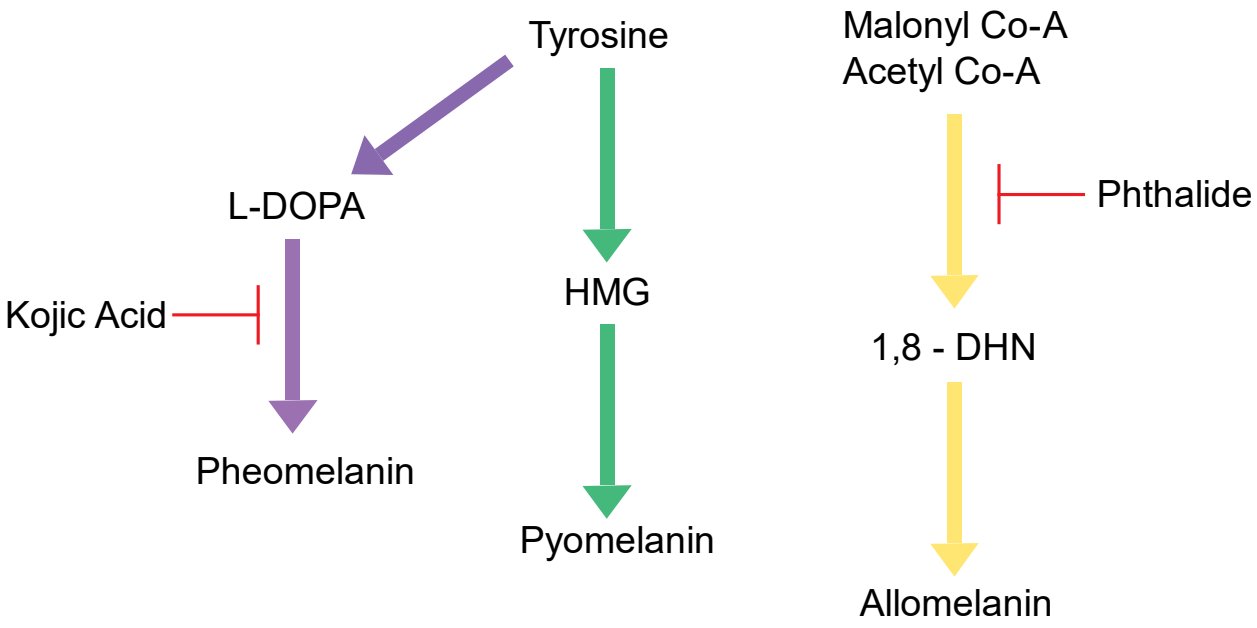

Figure 1: Visual summary of generalized fungal melanin production and the chemicals that block each pathway. Pheomelanin and Pyomelanin both use tyrosine as their starting reagent but have different biosynthesis pathways. Pheomelanin uses L-DOPA as a precursor to the final product and pyomelanin uses HMG as a precursor. Allomelanin's starting components are malonyl co-A and acetyl co-A, and its immediate precursor is 1,8-DHN. Kojic acid is a chemical blocker that blocks production of pheomelanin, and phthalide blocks production of allomelanin.

Table 1: Medias used and their compositions

Media Name	**Acronym**	**Composition (L^{-1})**
Malt Extract Agar Glucose	MAG	20 g Dextrose 20 g Malt Extract 2 g Peptone 1 mL Hutner's Trace Elements 1 mL Vitamin Mix 15 g Agar
Malt Extract Agar	MEA	20 g Dextrose 20 g Malt Extract 2 g Peptone 15 g Agar
Minimal	MN	10 g Dextrose 50 mL 20x Nitrate salts 1 mL Hutner's Trace Elements
Minimal + Vitamins	MNV	10 g Dextrose 50 mL 20x Nitrate salts 1 mL Hutner's Trace Elements 1 mL Vitamin Mix to MN
Minimal + N-acetyl Glucosamine	MN+NAG	10 g Dextrose 50 mL 20x Nitrate salts 1 mL Hutner's Trace Elements

		4.74 g N-Acetyl Glucosamine (21.43 mM)
Potato Dextrose Agar	PDA	24 g Potato dextrose powder 15 g agar (if not in potato powder)
Spider	Spider	20 g Nutrient Broth 20 g Mannitol 4 g K_2HPO_4 27 g Agar pH adjusted to 7.2 with NaOH
Yeast Extract Peptone Dextrose	YPD	20 g Dextrose 20 g Peptone 10 g Yeast Extract 20 g Agar
V8	V8	200 mL V8 Juice 2 g $CaCO_3$ 15 g Agar
Additives	**Volume/L**	**Composition**
20X Nitrate Salts/MN salts	1 L	120 g $NaNO_3$ (remove for "MN salts") 10.4 g KCl 10.4 g $MgSO_4$-$7H_2O$ 30.4 g KH_2PO_4
Hutner's Trace Elements	100 mL	2.2 g $ZnSO_4$-$7H_2O$ 1.1 g H_3BO_3 0.5 g $MnCl_2$-$4H_2O$ 0.5 g $FeSO_4$-$7H_2O$ 0.17 g $CoCL_2$-$6H_2O$ 0.16 g $CuSO_4$-$5H_2O$ 0.15 g Na_2MoO_4-$2H_2O$ 5 g EDTA (Na_4)
Vitamin Mix	100 mL	10 mg biotin 10 mg pyridoxin 10 mg thiamine 10 mg riboflavin 10 mg p-aminobenzoic acid (PABA) 10 mg nicotinic acid

Table 2: Nitrogen Sources, Concentrations, and Providers

Nitrogen Source	**Concentration**	**Catalog number**
No Nitrogen	N/A	N/A
Peptone	1% w/v	Fisher Brand: BP1420
L-Proline	100 mM	Sigma: P-0380
Ammonium tartrate	100 mM	Sigma: A2956
L-Serine	100 mM	Sigma: S4500
Sodium Nitrate	100 mM	Fisher Brand: S343
Glycine	100 mM	Fisher BioReagents: BP381

L-Glutamic acid	100 mM	Sigma: G1251
L-Aspartic acid	100 mM	Sigma: A9256
Urea	50 mM	Alfa Aesar: A12360

Table 3: Metals used and their concentration

Metal	Concentration	Catalog Number
$FeSO_4$	1 M	Fisher: I146
$CoCl_2$	0.5 M	Sigma: C-2644
$NiCl_2$	1.5 M	Sigma-aldrich: 223387
$CuCl_2$	1.5 M	Sigma: 203149
$CdCl_2$	10 mM	Fisher: 7790-84-3
$AgNO_3$	0.47 M	Alfa Aesar: 7761-88-8

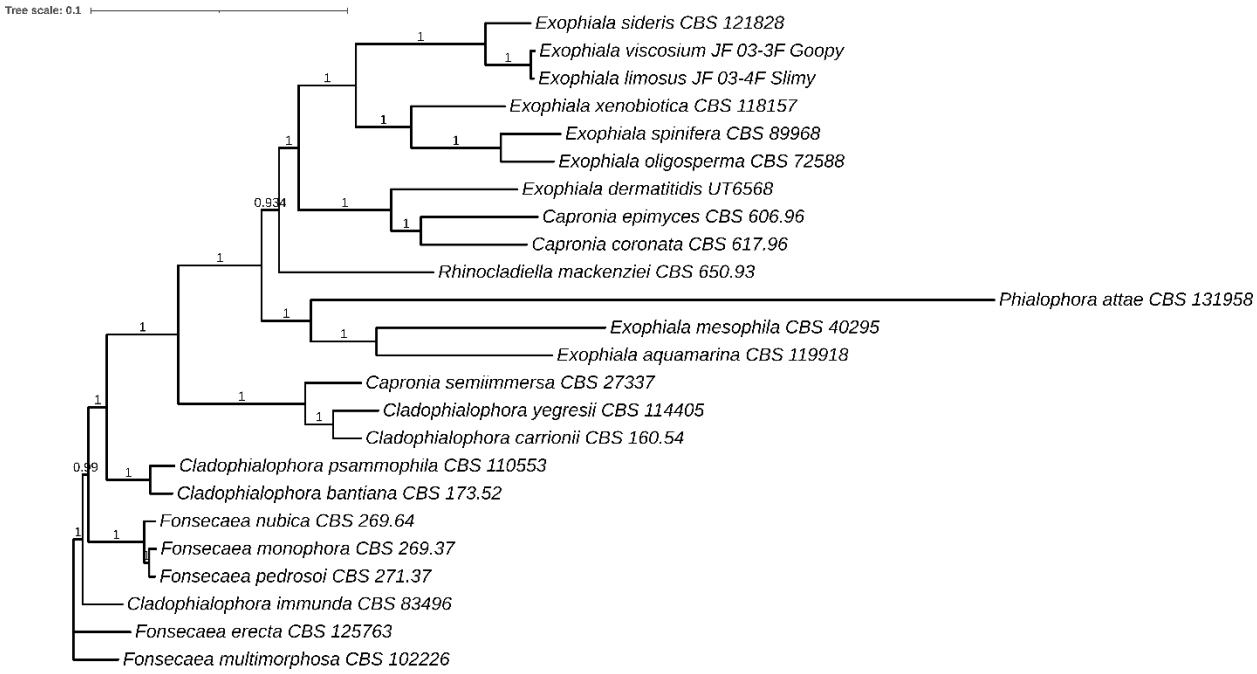

Figure 2: Protein sequence approximate maximum likelihood phylogenetic tree of taxa of the family Herpotrichiellaceae which have been whole genome sequenced and annotated. *E. viscosium* and *E. limosus* are shown to be closely related to *E. sideris*.

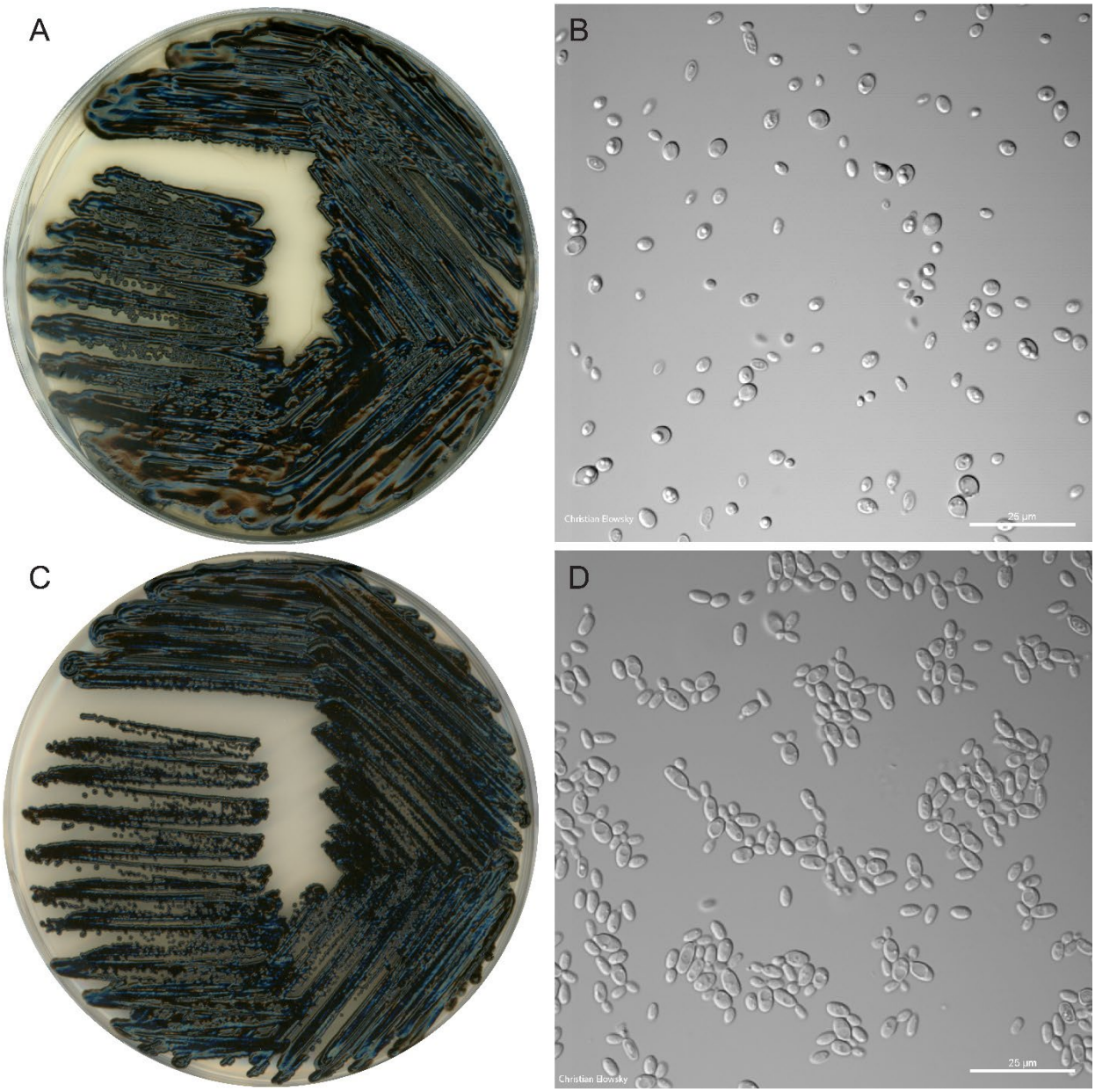

Figure 3: A) *E. viscosium* plate morphology; grown on an MEA plate for 10 days. *B) E. viscosium* cell morphology; grown in liquid MEA for 5 days; 60x objective lens. C) *E. limosus* plate morphology; grown on a MEA plate for 10 days. D) *E. limosus* cell morphology; grown in liquid MEA for 5 days; 60x objective lens. (Both plate photos and microscopy photos were taken by Christian Elowsky)

Table 4: Genome descriptions of the novel *Exophiala* species and close relatives

Genome Assembly statistics	*E. viscosium*	*E. limosus*	*E. sideris*	*E. spinifera*	*E. xenobiotica*	*E. oligosperma*	*E. dermatitidis*
Accession #s	PRJNA501636	PRJNA501637	PRJNA325799	PRJNA325800	PRJNA325801	PRJNA325798	PRJNA225511
Genome Assembly size (Mbp)	28.29	28.23	29.51	32.91	31.41	38.22	26.35

Sequencing read coverage depth	147.3x	147.8x	NA	NA	NA	NA	NA
Number of contigs	35	27	69	143	64	287	10
Number of scaffolds	30	17	5	28	15	143	10
Number of scaffolds >= 2Kbp	25	17	5	20	11	129	10
Scaffold N50	4	5	2	4	3	5	4
Scaffold L50 (Mbp)	2.24	2.89	7.9	3.79	5.04	3.39	3.62
Number of gaps	5	10	64	115	49	144	0
% of scaffold length in gaps	0.00%	0.00%	0.10%	0.10%	0.10%	0.80%	0.00%
Three largest Scaffolds (Mbp)	5.39, 4.56, 2.49	4.57, 3.58, 2.93	9.94, 7.90, 7.15	6.18, 3.93, 3.92	5.55, 5.20, 5.04	4.47, 4.29, 4.12	4.25, 4.22, 3.71
GC content (%)	51.91	49.26	49.73	49.42	51.89	50.99	51.74
Gene statistics							
Number of genes	11344	11358	11120	12049	13187	13234	9562
Gene length (bp, Average)	1840	1844	2044	1593	2072	2090	2237
Gene length (bp, Median)	1666	1671	1823	1415	1845	1879	1923
Transcript length (bp, Average)	1740	1746	1933	1483	1941	1949	2122
Transcript length (bp, Median)	1564	1574	1710	1311	1710	1735	1794
Exon length (bp, Average)	705	707	776	621	738	743	896
Exon length (bp, Median)	410	414	452	339	430	426	513
Intron length (bp, Average)	70	69	74	81	80	85	85
Intron length (bp, Median)	56	56	56	61	57	61	62
Protein length (aa, Average)	488	489	500	494	492	488	501
Protein length (aa, Median)	428	430	434	437	431	429	429
Exons per gene (Average)	2.47	2.47	2.49	2.39	2.63	2.62	2.37
Exons per gene (Median)	2	2	2	2	2	2	2

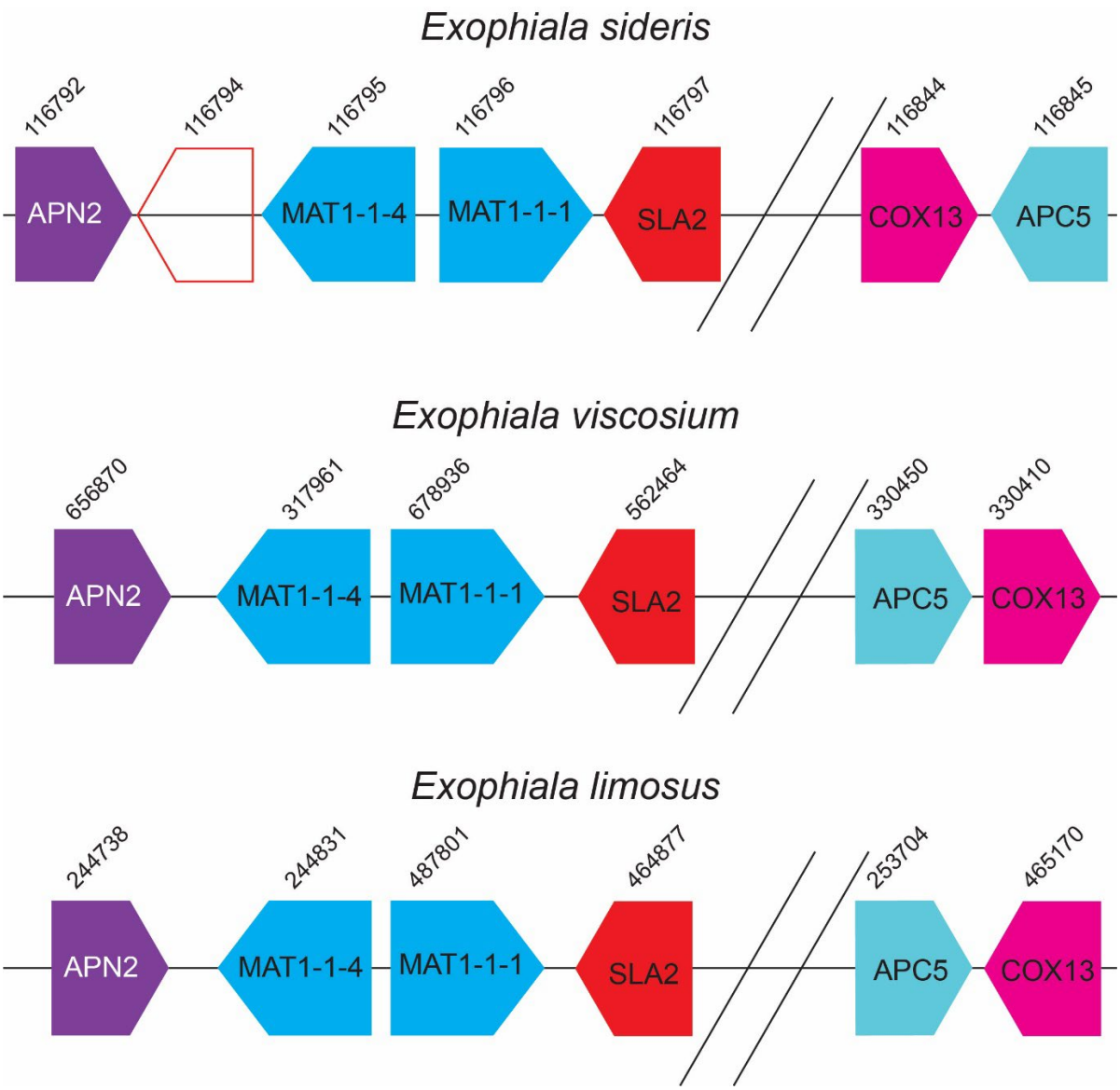

Figure 4: MAT loci gene order for *E. viscosium*, *E. limosus*, and *E. sideris*. In all three species the same genes are present within the MAT locus. *E. sideris* is indicated to have a hypothetical protein between APN2 and MAT1-1-4, whereas *E. viscosium and E. limosus* were not predicted to have that gene. Additionally, all three species have COX 13 and APC5 downstream of their mat loci, but the gene order or orientation is different amongst the three species.

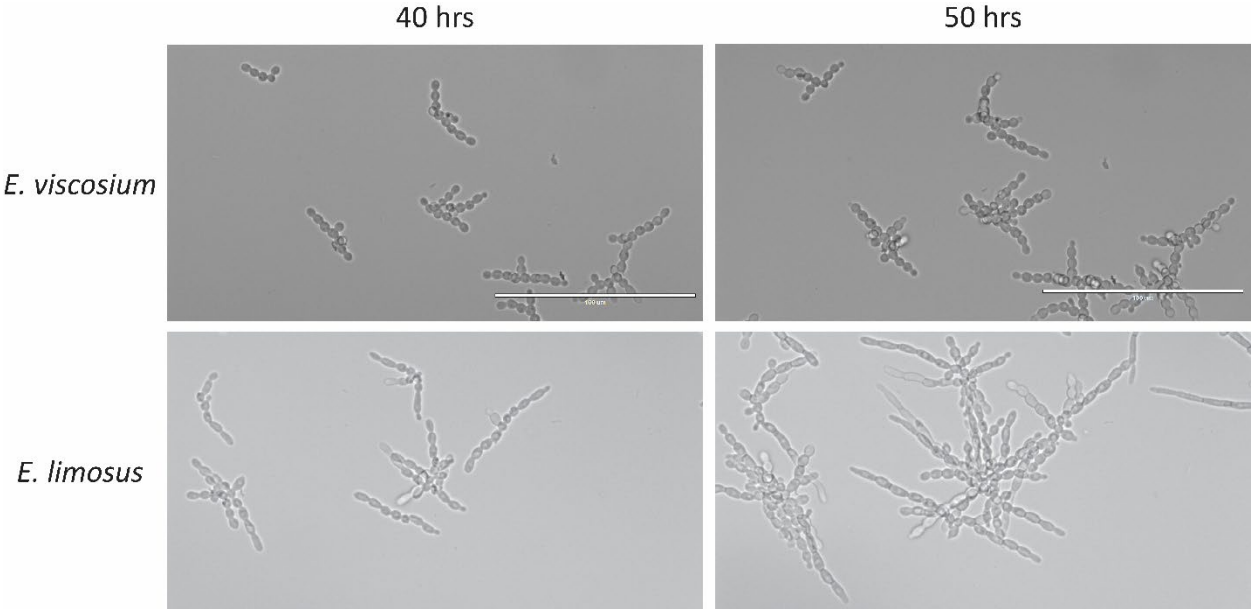

Figure 5: Budding styles of *E. viscosium* and *E. limosus*. Rate of budding is higher is E. limosus than in E. viscosium, as seen at the 50 hrs mark. Budding style is also different between the species, *E. viscosium* buds both distal polarly and proximal at close to a 90° angle, whereas *E. limosus* buds almost exclusively as a distal polar. *E. limosus*'s cells also elongate with every bud, forming almost hyphal-like structures at the 50 hr timepoint.

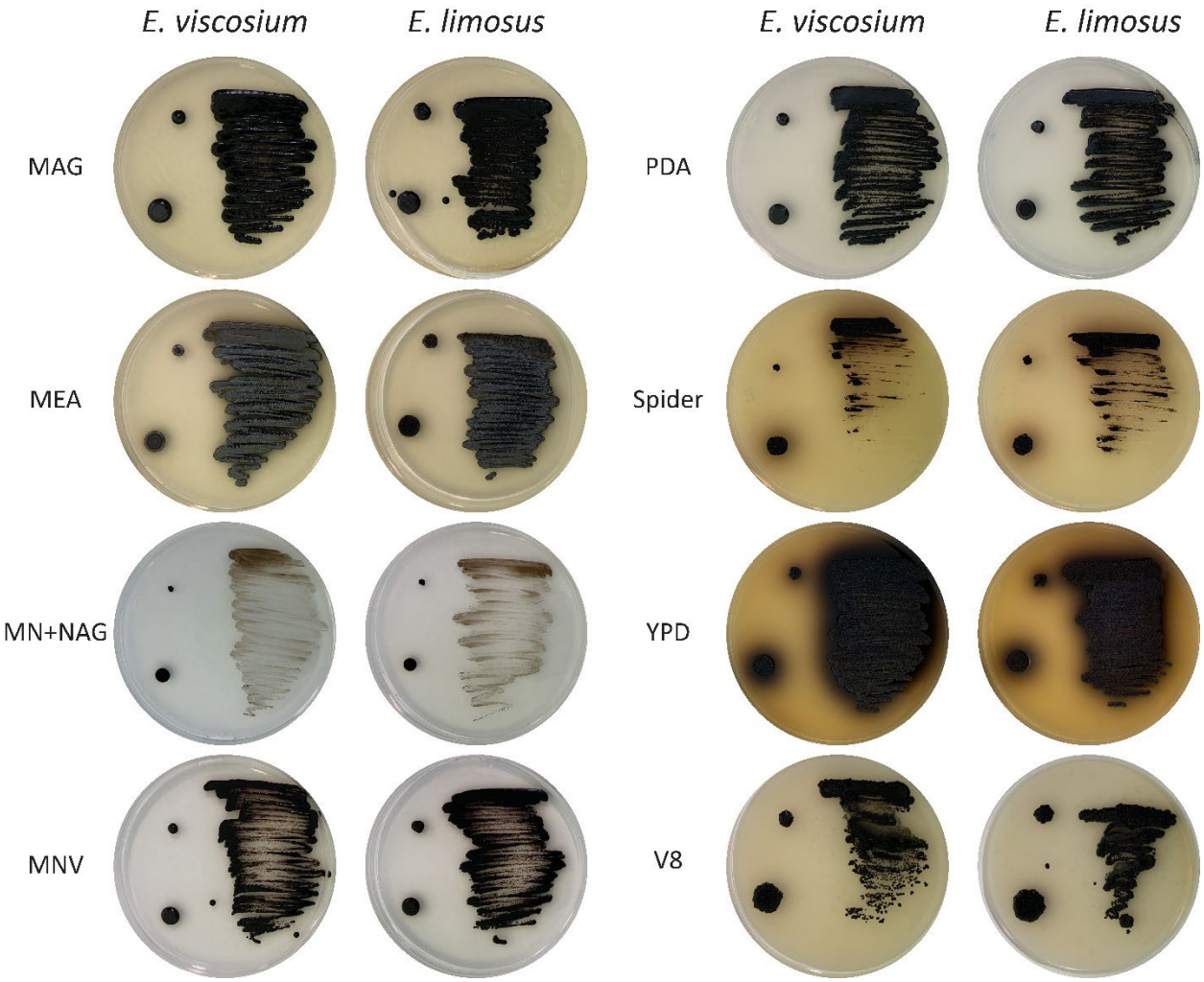

Figure 6: Growth of *E. viscosium* and *E. limosus* on eight different media types. Both species were capable of growth on all medias tested, but growth on MN+NAG showed the least amount of growth. PDA, MAG, and MNV allowed for very shiny and dark colonies to form in both species. Growth on V8 medium confirms potential for saprotrophic growth. Colorful secretions were observed on both Spider media and YPD for both species, though *E. viscosium* has more secretion into YPD than *E. limosus*.

Table 5: Carbon source utilization scores of *E. viscosium* and *E. limosus*

E. viscosium	D-galactose	D-sorbitol	Actidione (cycloheximide)	D-xylose	D-saccharose (sucrose)	D-ribose	N-acetyl-glucosamine	Glycerol	Lactic acid	L-rhamnose	L-arabinose	palatinose	D-cellobiose	Erythritol	D-rafinose	D-melibiose	D-maltose	sodium glucuronate	D-trehalose	D-melezitose	potassium 2-ketogluconate	potassium gluconate	methyl-aD-glucopyranoside	levulinic acid (leuvulinate)	D-mannitol	D-glucose	D-lactose	L-sorbose	Inositol	glucosamine	no substrate	Esculin ferric citrate
1	4	4	5	4	1	2	4	4	3	4	4	3	4	2	1	1	4	2	3	2	4	2	1	4	3	5	1	5	2	1	1	+
2	5	4	4	4	1	2	5	4	3	4	4	3	4	2	1	1	4	2	3	2	3	2	1	3	3	5	1	5	2	1	1	+
3	4	4	4	4	1	2	4	4	3	4	4	3	4	2	1	1	4	2	3	2	4	2	1	4	3	5	1	5	2	1	1	+

Avg	4.3	4.0	4.3	4.0	1.0	2.0	4.3	4.0	3.0	4.0	4.0	3.0	4.0	2.0	1.0	1.0	4.0	2.0	3.0	2.0	3.7	2.0	1.0	3.7	3.0	5.0	1.0	5.0	2.0	1.0	1.0	+
	+	+	+	+	-	V	+	+	V	+	+	V	+	V	-	-	+	V	V	V	+	V	-	+	V	+	-	+	V	-	-	+
E. limosus																																
1	4	5	4	4	2	2	4	4	3	4	4	4	4	1	1	1	4	2	4	2	3	2	1	3	3	5	1	5	2	2	1	+
2	4	5	4	4	2	2	4	4	3	4	4	4	4	2	1	1	4	2	3	2	3	2	1	4	3	5	1	5	2	2	1	+
3	4	5	4	4	2	3	4	4	3	4	4	4	4	2	1	1	4	2	4	2	4	2	1	3	4	5	1	5	2	1	1	+
Avg	4.0	5.0	4.0	4.0	2.0	2.3	4.0	4.0	3.0	4.0	4.0	4.0	4.0	1.7	1.0	1.0	4.0	2.0	3.7	2.0	3.3	2.0	1.0	3.3	3.3	5.0	1.0	5.0	2.0	1.7	1.0	+
	+	+	+	+	V	V	+	+	V	+	+	+	+	V	-	-	+	V	+	V	V	V	-	V	V	+	-	+	V	V	-	+

Figure 7: Growth of (A) *E. viscosium* and (B) *E. limosus* on C32 strips for determining carbon utilization. Both species were capable of using the same carbon sources, though some variations are seen. *E. limosus* was better at growing on palatinose, trehalose, potassium 2-ketogluconate, and mannitol than *E. viscosium*. *E. viscosium* was not better at growing on any carbon sources than *E. limosus*.

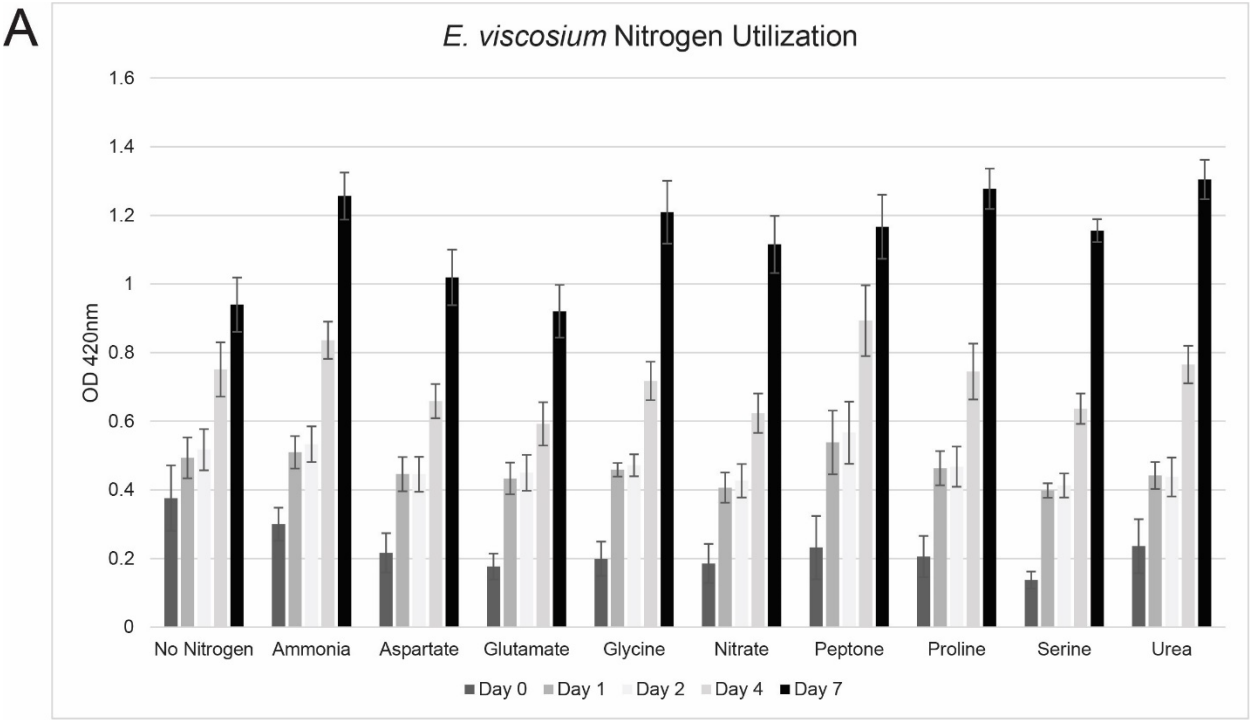

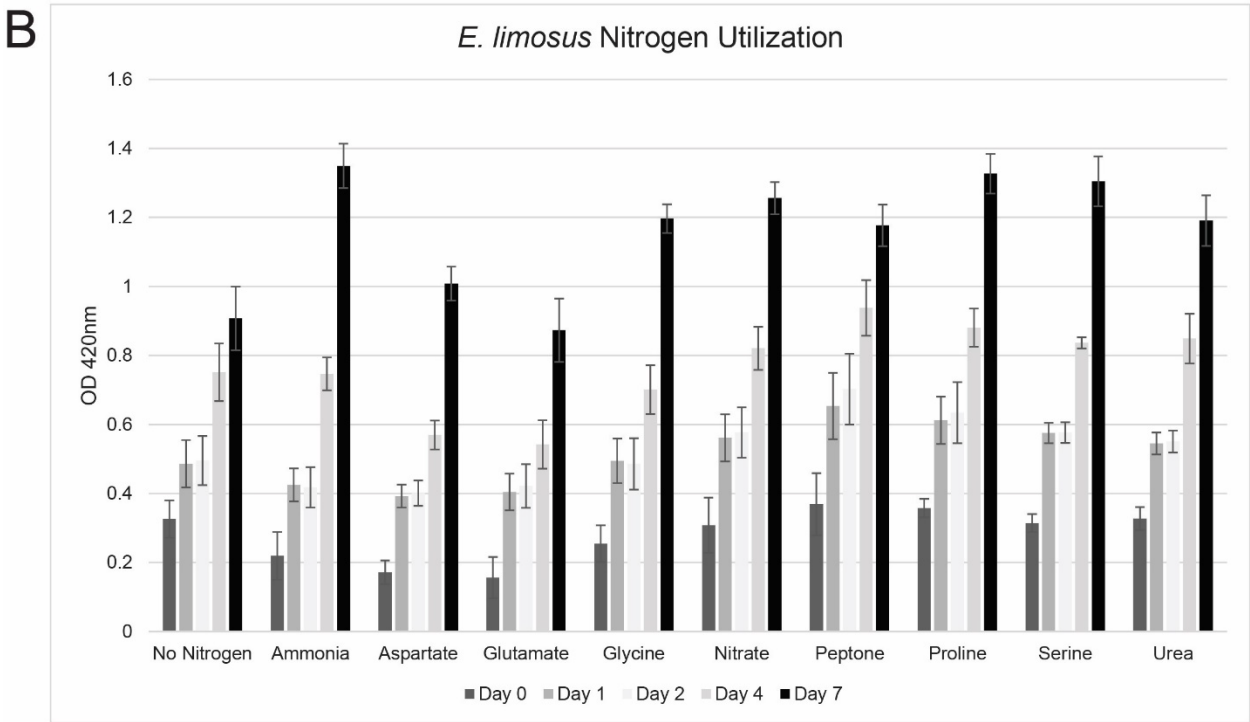

Figure 8: Nitrogen source utilization of *E. viscosium* and *E. limosus* in liquid culture. Neither species was capable of using aspartate or glutamate as a nitrogen source, as their growth amount were equivalent to no nitrogen. All other nitrogen sources tested were used by both species with varying preference. Ammonium was the preferred nitrogen source for *E. limosus*, and *E. viscosium* preferred urea and proline for nitrogen sources.

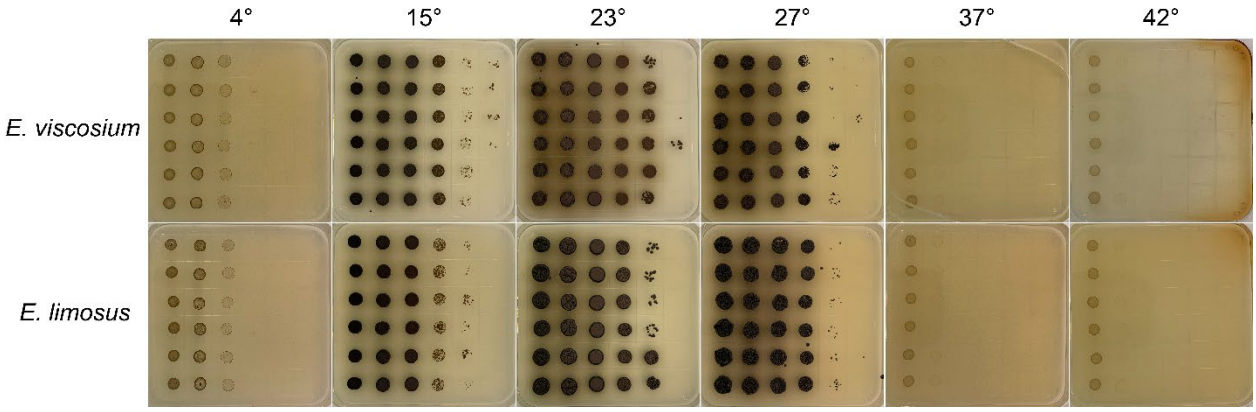

Figure 9: Growth of *E. viscosium* and *E. limosus* at varying temperatures. Neither species was capable of growth at or above 37° C, implying they are not human pathogens. Both species optimally grew at 23° C, but were capable of growth down to 4° C.

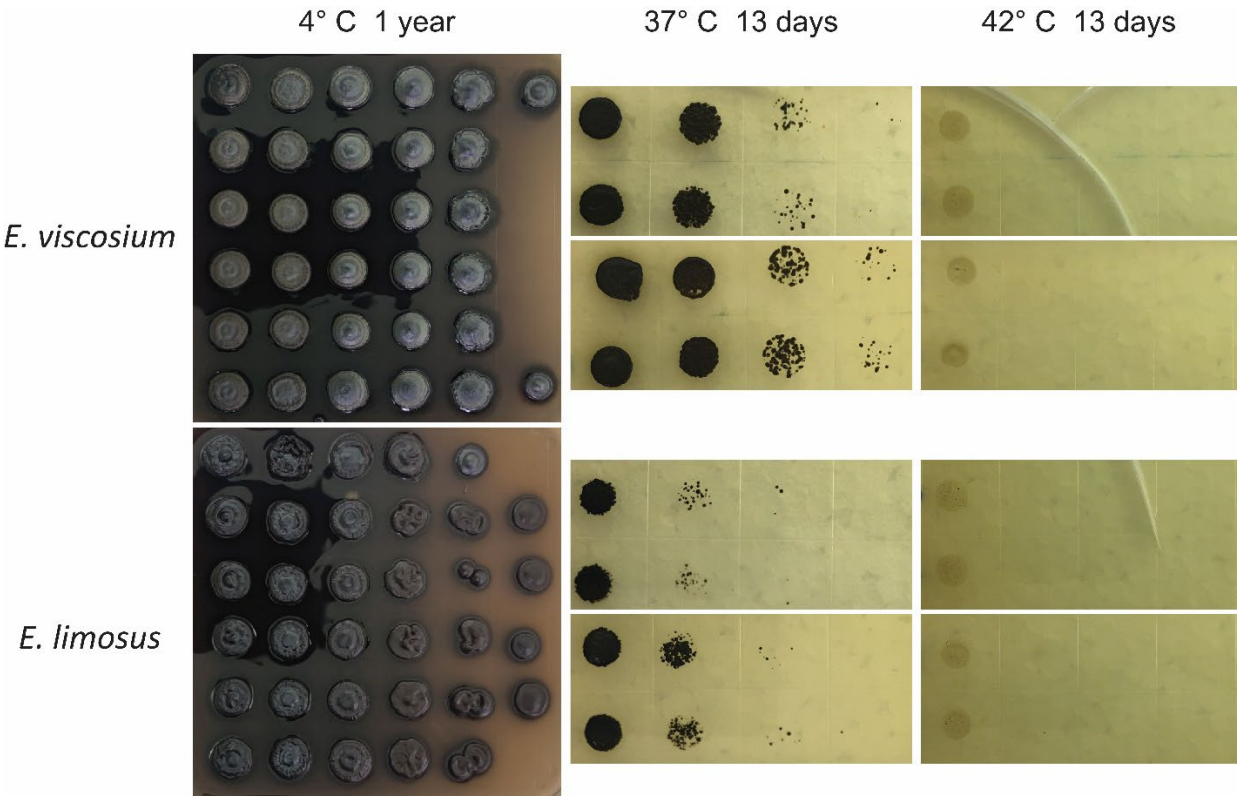

Figure 10: Growth of *E. viscosium* and *E. limosus* at the lowest and highest temperatures tested, after extended periods of time. Growth at 4° C continued for a year in both species, indicating that they can grow at these lower temperatures for extended periods of time. Additionally, we observed that while neither species was capable of active growth at 37° C it also was not too long of an exposure time to kill these cells. Whereas at 42° C neither species was capable of growth and was killed after 48 hrs of exposure.

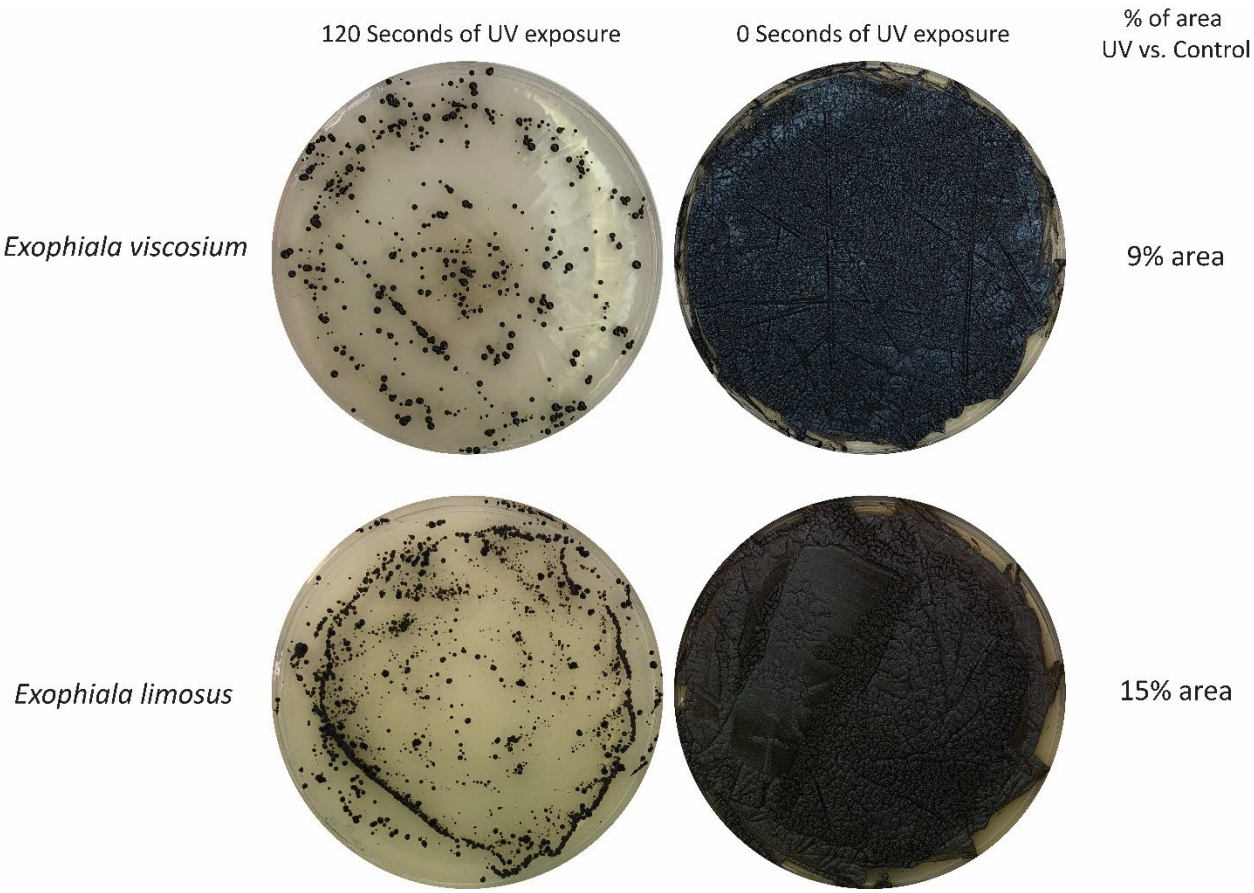

Figure 11: Difference in growth of *E. viscosium* and *E. limosus* with and without exposure to UV light. E. viscosium showed slightly less resistance to the UV exposure than E. limosus. Neither species was mutated from 120 seconds of UV exposure, normally *S. cerevisiae* and *E. dermatitidis* are incapable of growth after the same amount of UV exposure (data not shown).

Table 6: Diameter of the zone of clearing of E. viscosium, *E. limosus*, *E. dermatitidis*, and *S. cerevisiae* with various metals

Species	**$FeSO_4$ 1 M**	**$CoCl_2$ 0.5 M**	**$AgNO_3$ 0.47 M**	**$NiCl_2$ 1.5 M**	**$CuCl_2$ 1.5 M**	**$CdCl_2$ 10 mM**
E. viscosium	1.6 cm	1.5 cm	1.4 cm	3.9 cm	1.3 cm	4.5 cm
E. limosus	1.8 cm	1.8 cm	1.4 cm	4 cm	1.5 cm	3.9 cm
E. dermatitidis	1.3 cm	1 cm	1.5 cm	2 cm	2.5 cm	1.2 cm
S. cerevisiae	1 cm	1.9 cm	2 cm	2.1 cm	2 cm	2.5 cm

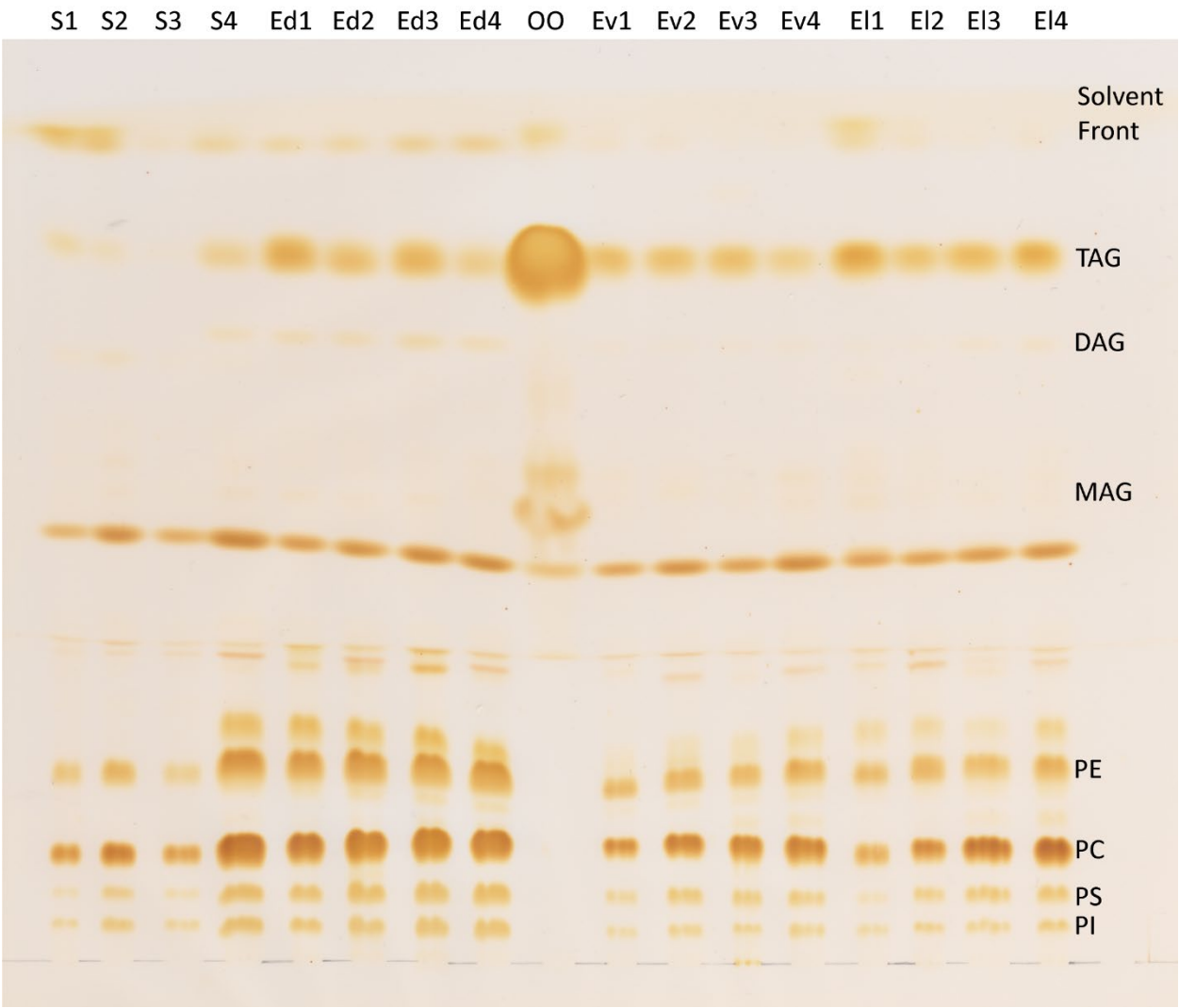

Figure 12: Lipid profile of *S. cerevisiae* (Sc), *E. dermatitidis* (Ed), *E. viscosium* (Ev), and *E. limosus* (El) using four different medias (1: MEA, 2: MEA + % peptone, 3: MEA + glycerol, 4: MEA + glycerol + % peptone). Differences in fermentable vs. non-fermentable carbon sources and amount of nitrogen source did not alter the amount or types of lipids produced by either *E. viscosium or E. limosus*. These fungi also showed no unique lipid production or any extreme accumulations of any lipids when compared to other fungi.

Table 7: Annotation of melanin biosynthetic genes for *E. viscosium* and *E. limosus*.

PKS/DHN/Allomelanin pathway		
Gene in *A. niger*	***E. viscosium* Homolog protein ID #**	***E. limosus* Homolog protein ID #**
Pks1	580617	463165
Ayg1	511449	494160
Arp2	676985	479993, 453709
Arp1	477931	210894
Abr2	603697, 153763	326274, 72468

Abr1	648725, 437535	258543, 441397
	387337, 648725	92776, 258543
	648725, 653857	258543, 102128
DOPA/Eumelanin/Pheomelanin pathway		
Gene in *A. niger*	***E. viscosium* Homolog protein ID #**	***E. limosus* Homolog protein ID #**
MelC2	140179, 643161	84855
	140179	84855
MelO	-	-
McoJ	571417	465594
McoM	571417	465594
McoD	437535	441397
McoG	437535	441397
McoF	437535	441397
McoN	653857, 649741	102128, 454148
McoI	653857, 649741	102128, 454148
L-Tyrosine degradation/Pyomelanin pathway		
Gene in *A. niger*	***E. viscosium* Homolog protein ID #**	***E. limosus* Homolog protein ID #**
Tat	606461	34310
hppD	623446	39306
hmgA	617354, 102643, 403121	430149, 483886, 431641
fahA	617341	148504
maiA	213100	198633

E. viscosium
E. limosus
10 mg/mL Kojic Acid
10 mM Phthalide
10 mg/mL Kojic Acid
10 mM Phthalide
E. viscosium
E. limosus
100 µg/mL Kojic Acid
100 µg/mL Phthalide
100 µg/mL Kojic Acid
100 µg/mL Phthalide

Figure 13

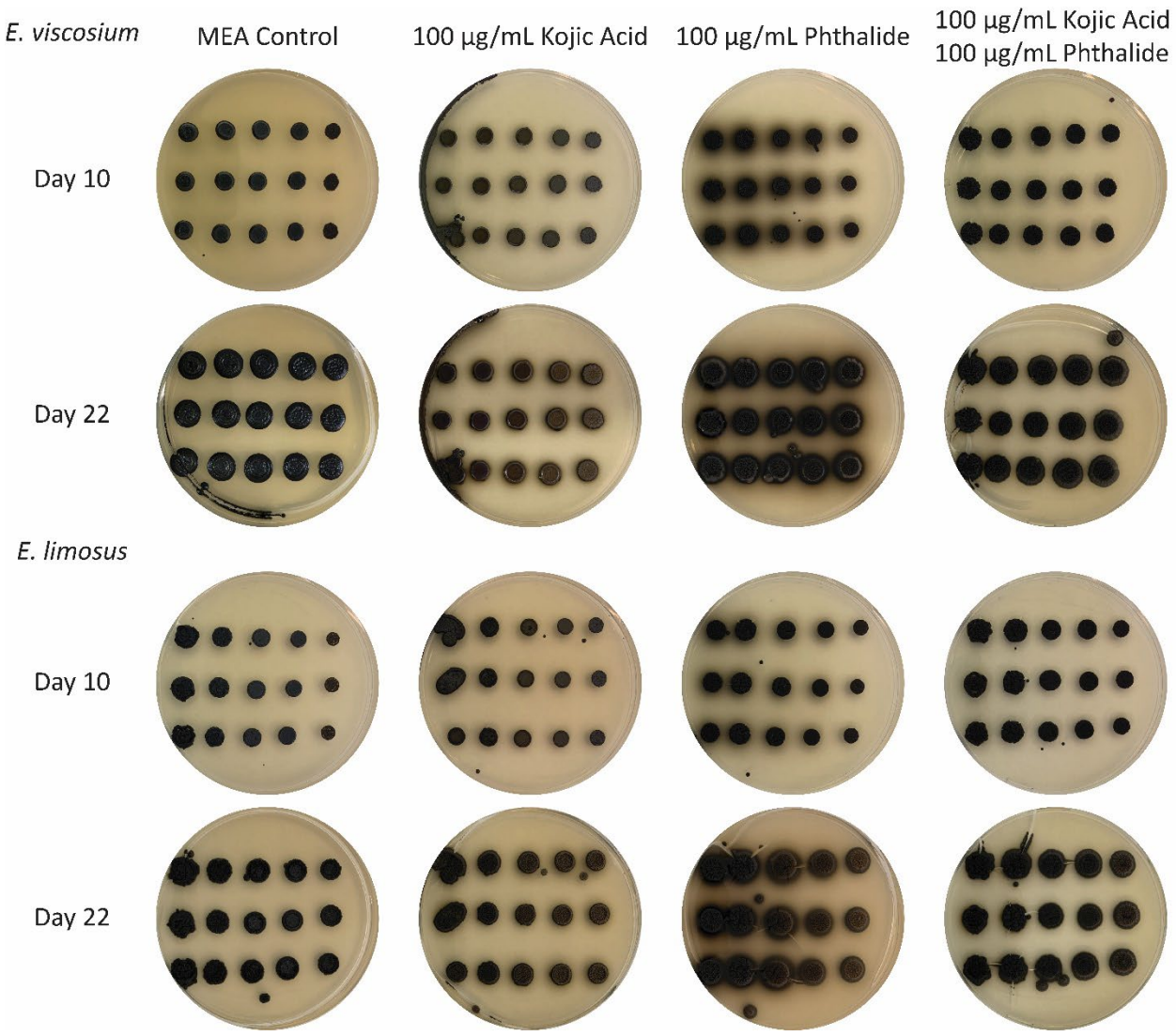

Figure 14: Growth of E. viscosium and E. limosus in the presence of melanin blockers kojic acid and phthalide. Neither chemcial melanin blocker was capable of blocking melanin production in either fungi even when both chemical blockers were used simultaneously. Additionally, use of phthalide on *E. viscosium* induced melanin secretion on a medium where this does not usually occur. The melanin halo around *E. viscosium*'s colonies on medium containing phthalide was replaced with hyphal growth after 22 days.

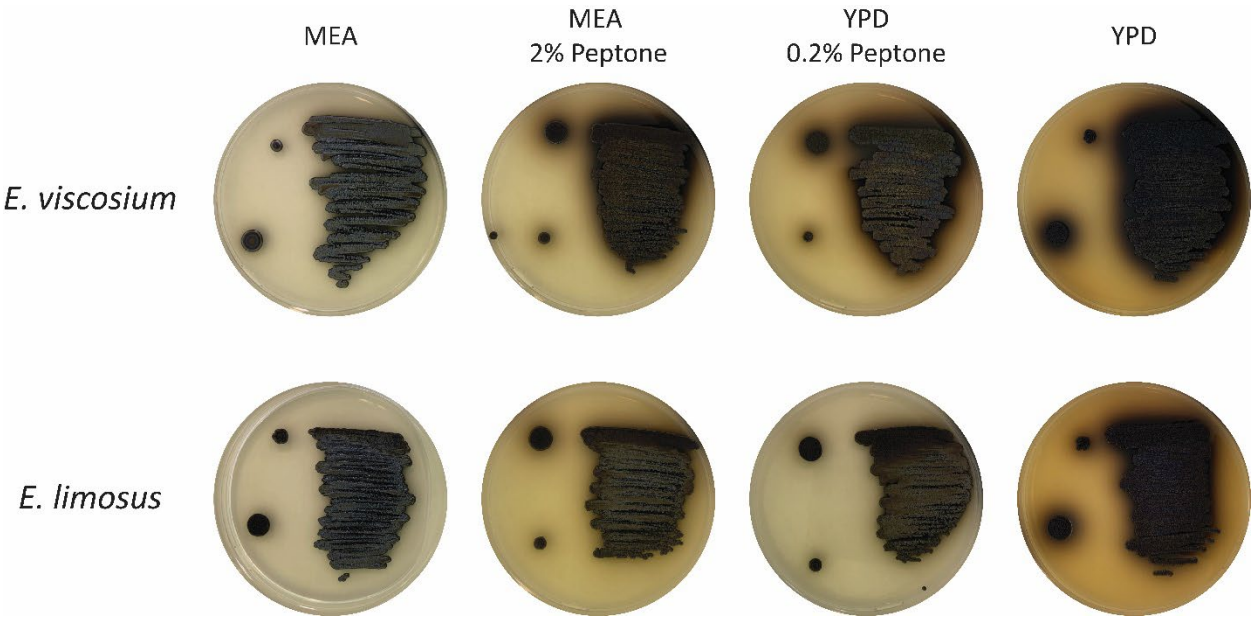

Figure 15: E. viscosium and *E. limosus* grown on MEA and YPD with different concentrations of peptone. *E. viscosium* is capable of melanin secretion on MEA with 2% peptone, which is the same amount of peptone in regular YPD. *E. limosus* was not as capable of secreting melanin in the MEA + 2% peptone, but there is a slight amount of secreted melanin. *E. viscosium* was also capable of secreting melanin on YPD with 0.2% peptone, indicating that yeast extract might have more available nitrogen than malt extract.

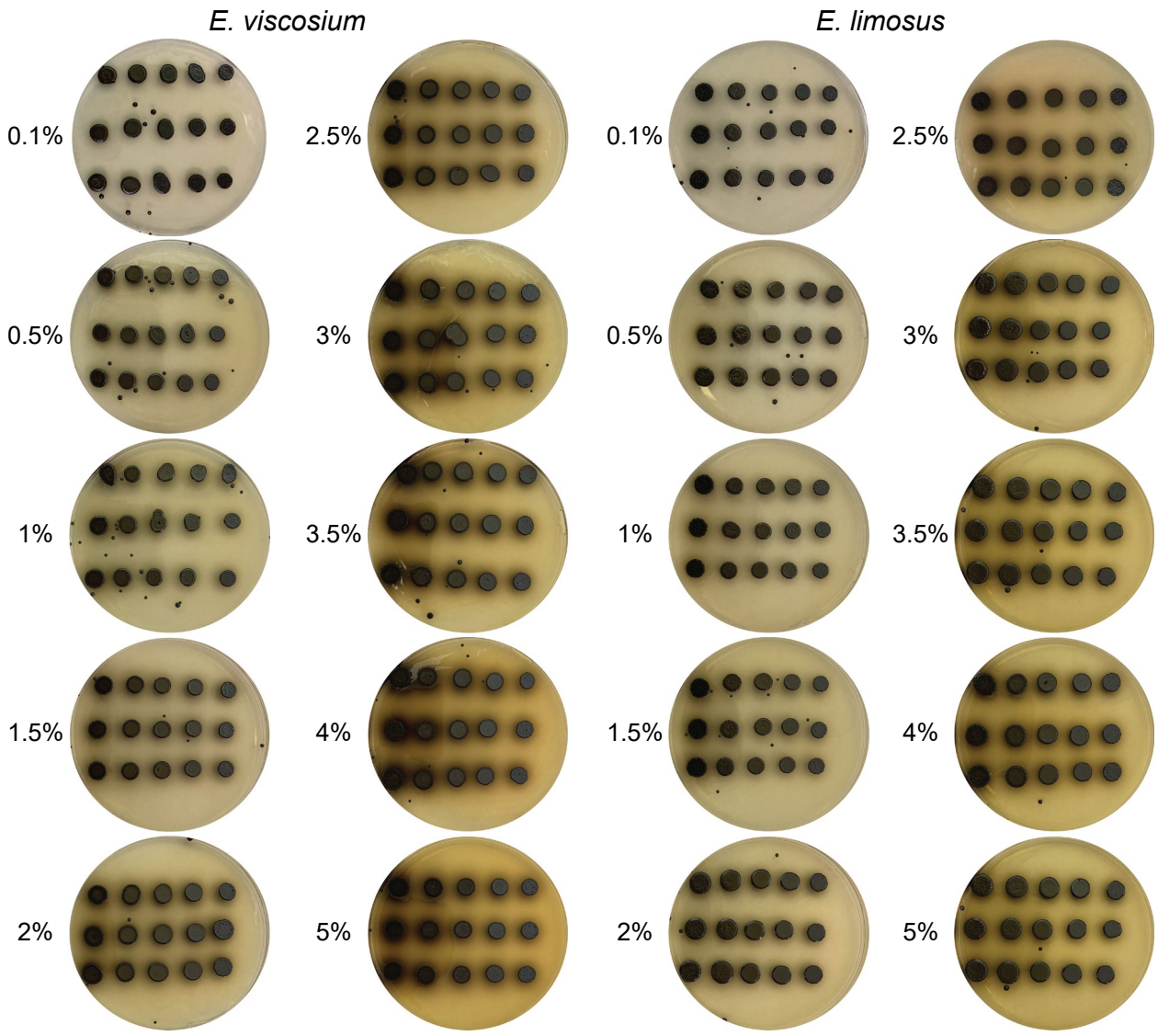

Figure 16: *E. viscosium* and *E. limosus* grown on MEA with increasing amounts of peptone. The higher the amount of peptone in the medium, the more melanin was secreted. *E. viscosium* started secreting melanin at 2%, and *E. limosus* at 4%.

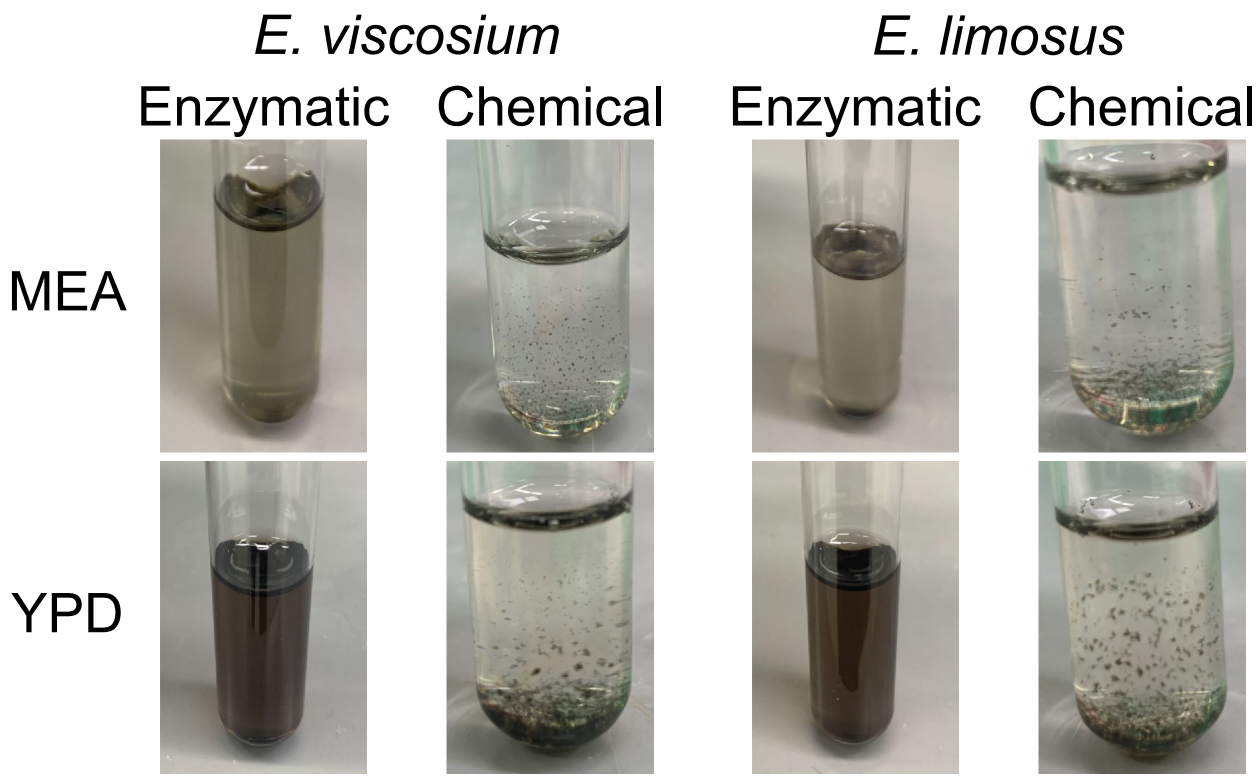

Figure 17: Extraction of melanin from supernatants of *E. viscosium* and *E. limosus* using both enzymatic and chemical methods described in (Pralea et al., 2019). Enzymatic extraction methods were incapable of extracting all the melanin, leaving behind a dark supernatant in the last step. However, melanin extracted by chemical extraction methods had complete extraction of the secreted melanin.

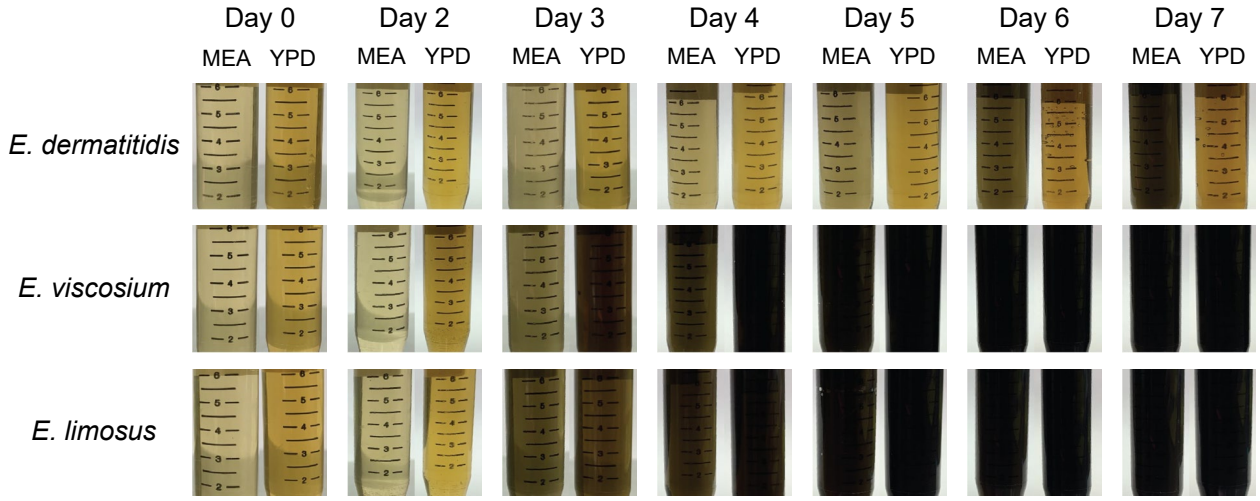

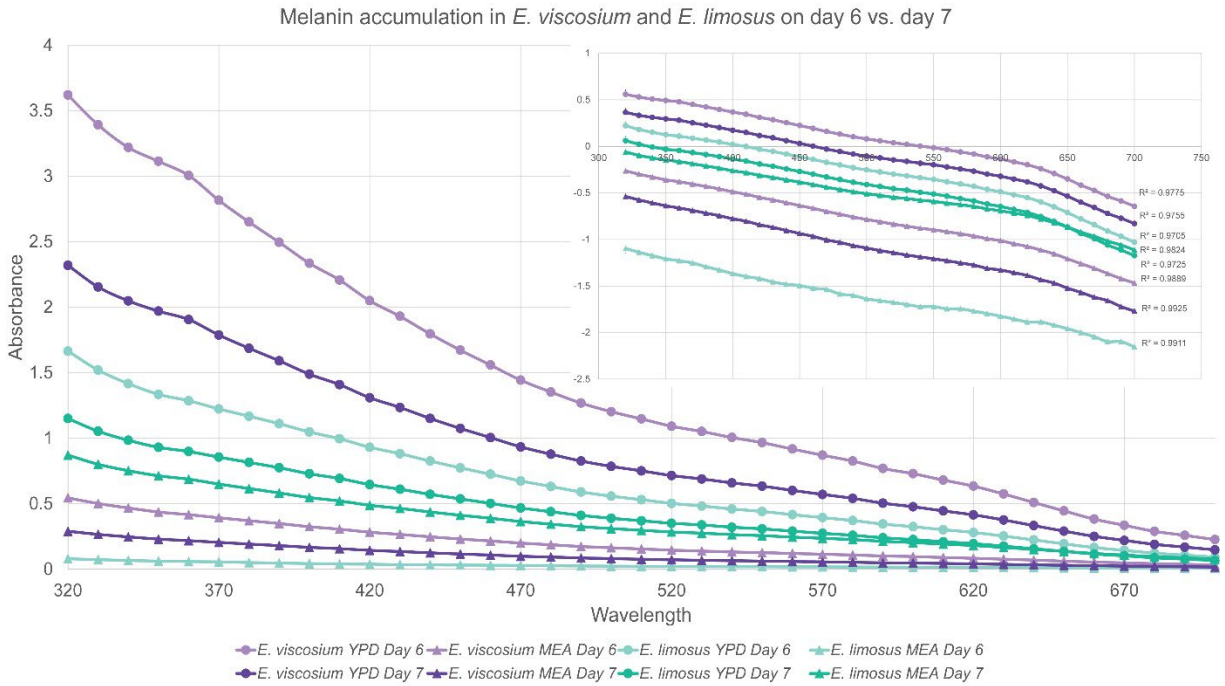

Figure 19: Day 7 results of daily melanin extraction from *E. viscosium*, *E. limosus*, and *E. dermatitidis*. All samples display typical melanin properties with full spectrum light, in that all samples have a linear regression with an R2 value of 0.97 or higher. The sample with the highest amount of secreted melanin on day 7 was *E. viscosium* in YPD. Both *E. viscosium* and *E. limosus* had more secreted melanin when grown on YPD as opposed to MEA which showed lower melanin secretion for both species. *E. dermatitidis* on the other hand had the highest amount of melanin in the supernatant in MEA than on YPD.

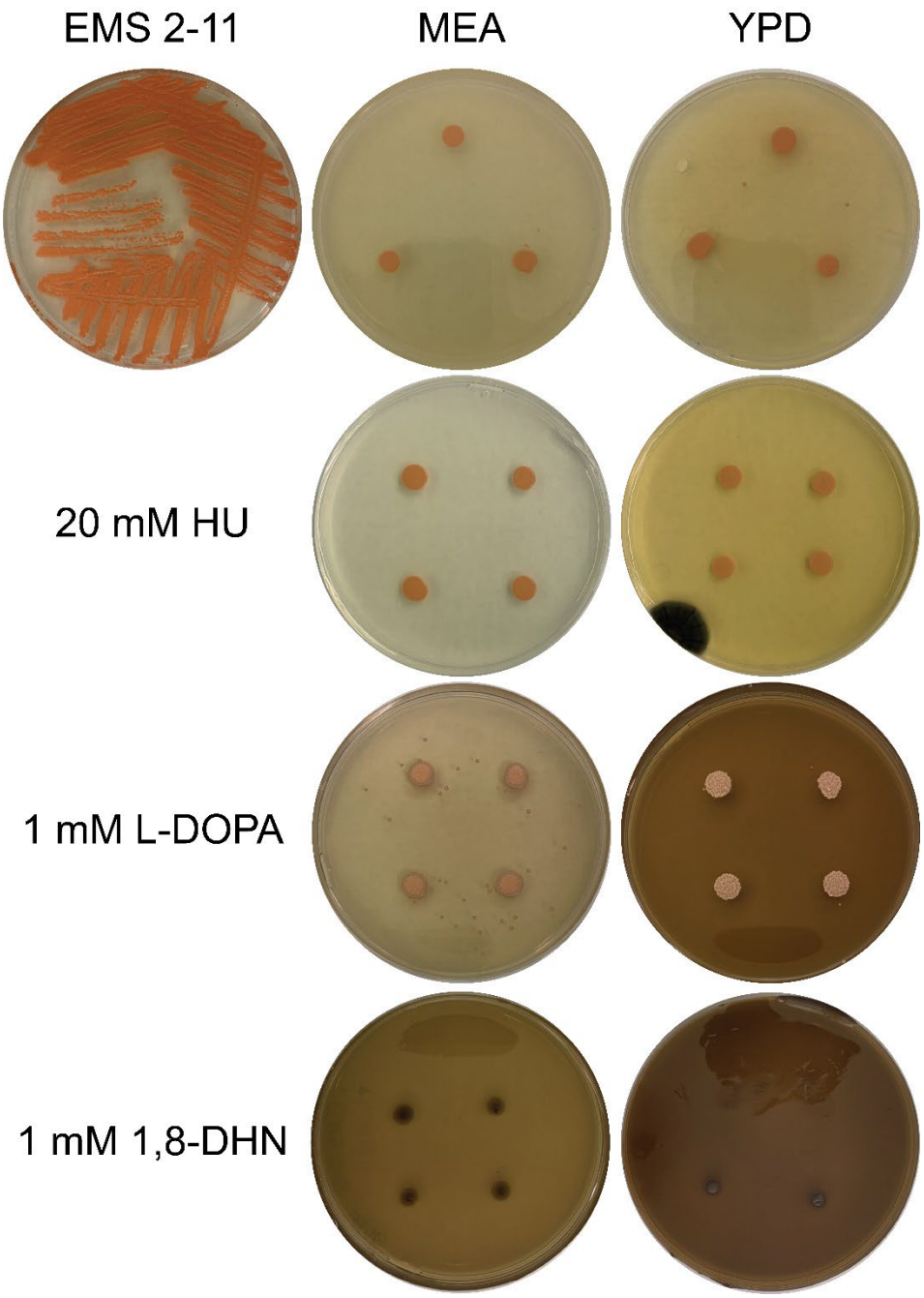

Figure 20: Phenotype of the EMS 2-11 mutant of *E. limosus* with pks1 nonsense mutation, causing melanin production to be stopped hence the pink coloration. Attempts to recover melanin production were done with Hydroxyurea (HU), L-DOPA, and 1,8-DHN. Neither HU or DOPA was able to recover the melanin in the mutant, however 1,8-DHN was able to recover melanin production in this mutant.